DE88002432

NOVEL EXPERIMENTAL STUDIES FOR COAL LIQUEFACTION: QUARTERLY PROGRESS REPORT, JULY 1, 1987-SEPTEMBER 30, 1987

PITTSBURGH UNIV., PA

1987

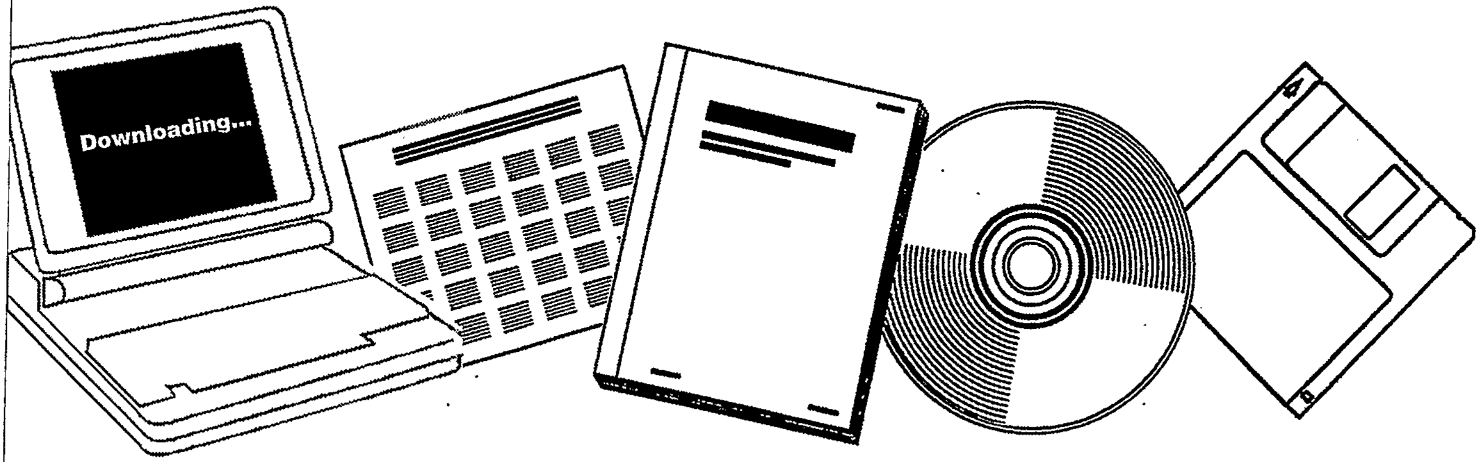

One Source. One Search. One Solution.

NTIS

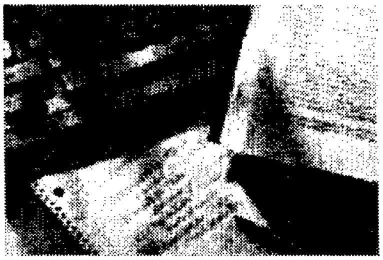

Providing Permanent, Easy Access to U.S. Government Information

National Technical Information Service is the nation's largest repository and disseminator of government-initiated scientific, technical, engineering, and related business information. The NTIS collection includes almost 3,000,000 information products in a variety of formats: electronic download, online access, CD-ROM, magnetic tape, diskette, multimedia, microfiche and paper.

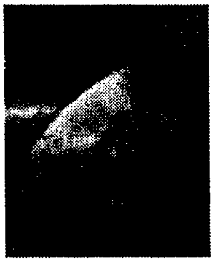

Search the NTIS Database from 1990 forward

NTIS has upgraded its bibliographic database system and has made all entries since 1990 searchable on **www.ntis.gov.** You now have access to information on more than 600,000 government research information products from this web site.

Link to Full Text Documents at Government Web Sites

Because many Government agencies have their most recent reports available on their own web site, we have added links directly to these reports. When available, you will see a link on the right side of the bibliographic screen.

Download Publications (1997 - Present)

NTIS can now provides the full text of reports as downloadable PDF files. This means that when an agency stops maintaining a report on the web, NTIS will offer a downloadable version. There is a nominal fee for each download for most publications.

For more information visit our website:

www.ntis.gov

U.S. DEPARTMENT OF COMMERCE
Technology Administration
National Technical Information Service
Springfield, VA 22161

DOE/PC/71257

Quarterly Progress Report

DOE/PC/71257--T13

DE88 002432

NOVEL EXPERIMENTAL STUDIES FOR COAL LIQUEFACTION

Gerald D. Holder
John W. Tierney

University of Pittsburgh
Pittsburgh, PA 15261

Prepared for the Department of Energy
Contract No. De-FG22-84PC71257

July 1, 1987 to September 30, 1987

NOVEL EXPERIMENTAL STUDIES FOR COAL LIQUEFACTION

Research is being carried out in this project in two areas which are of interest to ongoing investigations at the Pittsburgh Energy Technology Center (PETC). They are: (a) thermal behavior of slurry reactors used for indirect coal liquefaction, and (b) coal liquefaction under supercritical conditions. The current status of each of these tasks is summarized in this report.

CONTENTS

LIST OF FIGURES

LIST OF TABLES

TASK 1: THERMAL BEHAVIOR OF SLURRY REACTORS USED FOR INDIRECT COAL LIQUEFACTION

The conversion of synthesis gas to liquid products is usually carried out with the reactants in the gas phase and a solid catalyst. Because of relatively poor heat transfer from the gas to the solid, the exothermic heat of reaction is difficult to remove, and care must be taken to prevent the catalyst from overheating with loss of selectivity and activity. Slurry reactors in which the catalyst is suspended in a liquid medium and the gases are bubbled through the slurry have intrinsically better heat transfer characteristics and appear promising for indirect liquefaction processes.

1.1 Scope of Work

In Task 1 of this project, the use of a slurry reactor for indirect coal liquefaction is being studied. Work is being done using two indirect liquefaction routes involving synthesis gas - the Fischer-Tropsch reaction and the two-step conversion to methanol via methyl formate.

1.2 Results and Highlights

Experimental work and data analysis for the two-step methanol synthesis in a single slurry reactor were continued during the quarter. Experimental work included measurements of the effect of CO_2 on the simultaneous two-step reaction; measurement of the equilibrium concentration in the methanol-methyl formate-CO system; and identification of by-products that have been obtained in the simultaneous two-step process. Preparations were made for additional experimental measurements of heat effects in the Fischer-Tropsch reaction in a slurry reactor, and a modeling study was initiated by Dr. Shah to identify the important factors in the thermal behavior of slurry reactors for the Fischer-Tropsch synthesis. Details of each of these actvities are given below.

1.3 Future Work

During the next quarter work will continue on analysis of data obtained for the simultaneous two-step synthesis of methanol. Experimental work will include the measurement of the effect of carbon dioxide on the carbonylation reaction.

A new computer control system is being installed for the reactor, and will be used to obtain measurements of the heat effect in the Fischer-Tropsch synthesis. Work will also continue at the University of Tulsa on modeling of the Fischer-Tropsch reaction in a slurry reactor.

1.4 Effect of CO_2 on the Simultaneous Two-Step Reaction

It is well known that CO_2 plays an important role in the gas phase methanol synthesis. It is common practice to add 6 to 8% to the feed gases. As we have previously reported, the hydrogenolysis reaction using G-89 catalyst is poisoned by the addition of CO_2. With 0.6% of CO_2 in the feed gas there was a sharp drop in reaction rate. After 30 minutes the rate was reduced by 36%. Larger amounts of CO_2 in the feed gas produced larger decreases. Since we have found as much as 2% CO_2 in the product gases for the simultaneous two-step reaction even when there is none in the feed, a series of experiments were carried out to investigate the role of CO_2 in the simultaneous two-step process.

The one liter batch autoclave described in previous reports was used. The reaction temperature was 160°C and the pressure was 625 psig. The autoclave was charged with 500 cc of methanol, 20 gms of G-89 hydrogenolysis catalyst, and 15 gms of potassium methoxide, the carbonylation catalyst. A continuous gas feed of 324 cc/min was used with a H_2/CO ratio of three. These are the conditions which

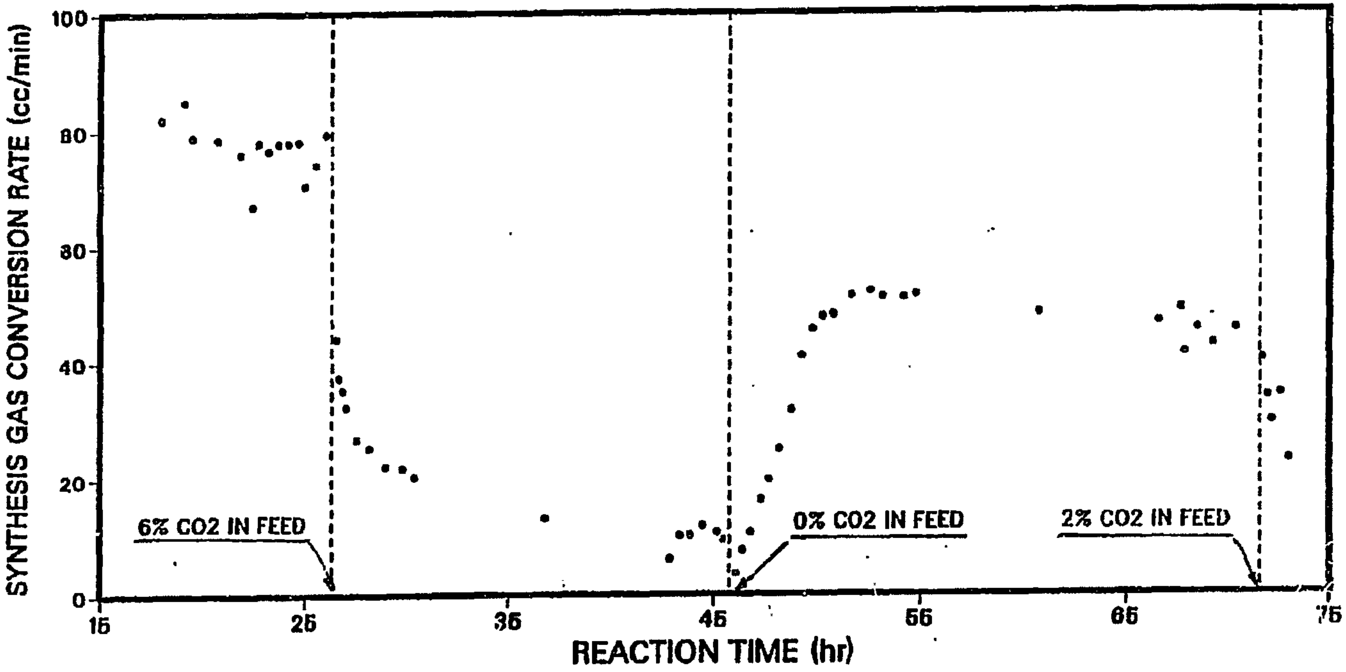

Figure 1. Effect of CO_2 on Synthesis Gas (H_2 + CO) Conversion

gave the highest methanol production in previous experiments. The reaction was carried out for 26 hours to insure that steady state was reached, and then 6% CO_2 was added to the feed. After 20 hours the CO_2 addition was discontinued, and the feed contained only CO and H_2. After 26 more hours, CO_2 was again added but with a concentration of 2%. The experiment was discontinued after 2 hours because of plugging in the reactor feed line, located at the reactor bottom.

The synthesis gas conversion rate is plotted against time in Figure 1. For the first 26 hours when there was no CO_2 addition, the conversion decreases slowly to about 74 cc/min. This is the same behavior that we have seen before. However, a very sharp decrease in conversion occurs when CO_2 is introduced, and in the next 20 hours the rate decreases to 10 cc/min. Then CO_2 is removed from the feed; the rate increases; and after 10 hours is 51 cc/min. This latter is approximately the conversion rate expected after 55 hours when there is no CO_2 addition but taking into account the normal decrease in conversion with time which has been seen before. At 72 hours, CO_2 addition was renewed but at a lower concentration, and again the conversion decreases but not as rapidly as when 6% CO_2 was used.

It is evident that CO_2 poisons one or both of the catalysts. However, the effect is reversible, since the conversion rate recovered when the CO_2 was removed. This is an important result for commercial application of this reaction because it indicates that permanent damage to the catalyst would not result from accidental introduction of CO_2 into the system. A possible mechanism for this poisoning is blocking of active sites on the heterogeneous catalyst by adsorption of CO_2. Since we know from previous experiments that the hydrogenolysis reaction carried out alone is poisoned, it is likely that this is the mechanism for the poisoning in the simultaneous reaction. However, we have not measured the effect of CO_2 on the carbonylation reaction carried out alone. We plan to do this during the next quarter.

Measurements of liquid composition were made during the run and showed that the methyl formate concentration during the run did not change and remained at the equilibrium value. This would seem to imply that the carbonylation reaction was not affected by CO_2. However, the conversion rate dropped to a very low value during CO_2 additions, and the failure to observe changes in methyl formate composition may be due to the low rate of the hydrogenolysis reaction.

About 1.4% of CO_2 was present in the product gases before any CO_2 was added to the reaction, and this CO_2 must result from side reactions. The source of this CO_2 is not known and is being investigated. It seems likely that CO_2 is at least partially responsible for the slow decrease in activity noted previously.

The concentration of another by-product, dimethylether (DME), was monitored during the run. The mole fractions in the gas phrase are plotted in Figure 2. The production of DME follows the same pattern as that of conversion rate shown in Figure 1. The DME was previously observed as a by-product for the carbonylation reaction and not for the hydrogenolysis reaction when each is carried out separately.

Hydrogen and CO are consumed in the ratio of 2/1 for the simultaneous two-step process when methanol is the only product. It was observed that the ratio changed from 2/1 to 6/1 when CO_2 was added to the feed. The explanation for this is not known and is being further studied.

1.5 Equilibrium Measurements for Carbonylation Reaction

The equilibrium concentrations predicted by the rate equation for carbonylation (Quarterly Report, July-September, 1986) do not accurately predict

$$r_1 = 4.11\times10^7 \exp(-10126/T) C_{Cata,1} C_{MeOH} P_{CO}$$

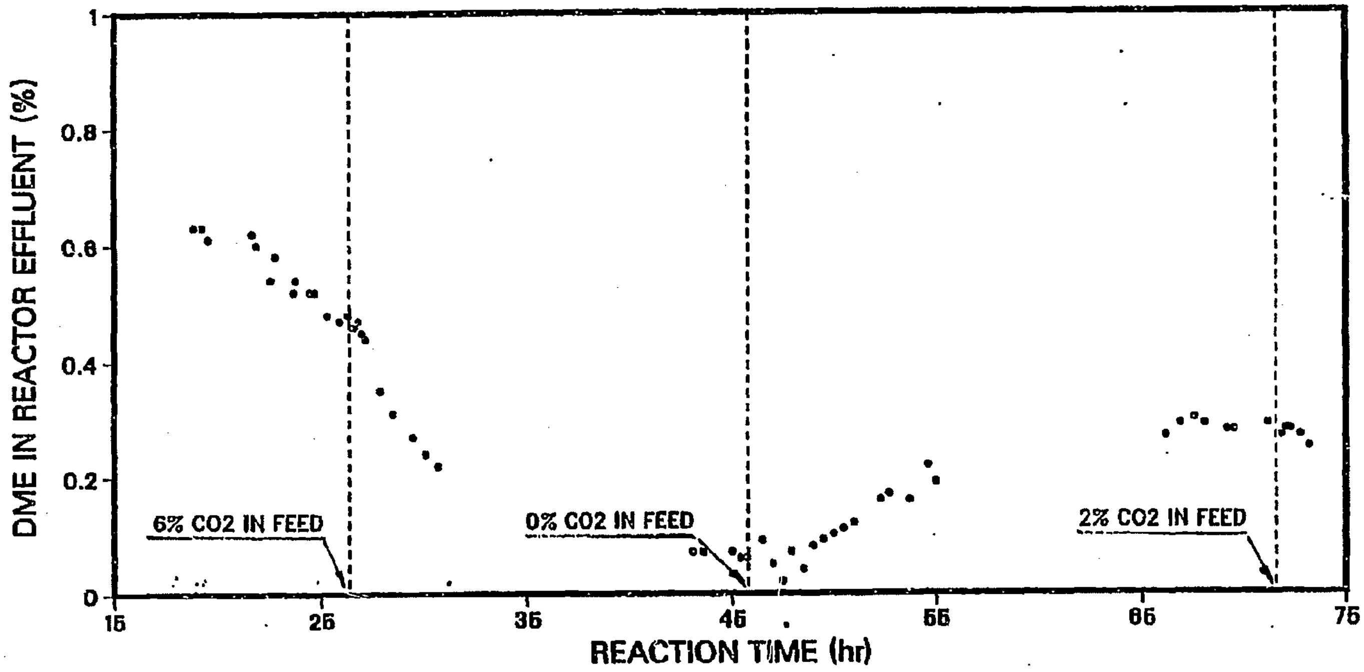

Figure 2. Effect of CO_2 on DME Concentration in the Reactor Effluent

$$-1.70\times10^{17}\ \exp(-16788/T)C_{Cata,1}C_{MeF} \qquad (1)$$

the equilibrium concentrations measured for the simultaneous reaction. The reason for this is that the rate equation was developed using data at conditions where the reverse reaction rate was small - less than 10% of the forward rate. By definition, at equilibrium the rates are equal, and small errors in the reverse rate can lead to large changes in the predicted equilibrium concentrations. For the simultaneous two step reaction, the carbonylation reaction is close to equilibrium, so accurate equilibrium measurements are necessary, and a series of experiments were carried out to determine the equilibrium composition as a function of temperature from 60 to 180°C.

The measurements were made in the one liter autoclave. Methanol, CO methyl formate, and potassium methoxide catalyst were charged to the reactor and heated to the desired temperature with a stirrer speed of 1400 rpm. The pressure was monitored and when constant for more than an hour, a liquid sample was taken and analyzed. CO_2 and DME were observed as by-products. A total of 32 data points were taken and correlated by the equation:

$$K_e = C_{MeF}/C_{MeOH}P_{CO} \qquad (2)$$

where C_{MeF} and C_{MeOH} are methyl formate and methanol concentrations in mole/liter and P_{CO} is the partial pressure of CO in atm. Linear regression was used to correlate the equilibrium ratio (K_e) with temperature and the following equation was obtained:

$$\ln(K_e) = -14.90 + 3780./T \qquad (3)$$

The correlation coefficient was 0.957.

The reverse equation constant determined from the forward rate equation (1) and the equilibrium ratio is:

$$r_r = 1.22\text{x}10^{14} \exp(-13906./T) \quad (4)$$

This is different from the one obtained from curve fitting method. The reverse rate in Equation (1) was obtained at low MeF concentrations far from equilibrium at low temperatures, while equation 4 was obtained from equilibrium data. Equation 1 is recommended for low MeF concentrations far from equilibrium. At conditions near equilibrium a combination of the forward rate from equation 1 and the equilibrium ratio from equation 3 is recommended.

$$r_1 = 4.11\text{x}10^7 \exp(10126/T) C_{Cata,1}(C_{MeOH}P_{CO} - C_{MeF}/K_e) \quad (5)$$

1.6 By-products Analysis in the Two-Step Synthesis

Gas chromatograms of typical gas and liquid samples are shown in Figure 3. A 6'x1/8" Porapak Q 80/100 mesh column was used at a constant temperature of 130°C with injection and detector temperatures of 200°C. The carrier He flow rate was 25 cc/min for each column at room condition. Besides CO (retention time of about 0.27), methanol (retention time from 2.8 to 3.8) and methyl formate (retention time from 4.5 to 4.8) three unidentified peaks were observed. Two liquid samples were sent to Pittsburgh Energy Technology Center (PETC) and to the University of Pittsburgh Applied Research Center (UPARC) for analysis. A gas chromatograph and a mass spectrograph were used in series. Each laboratory

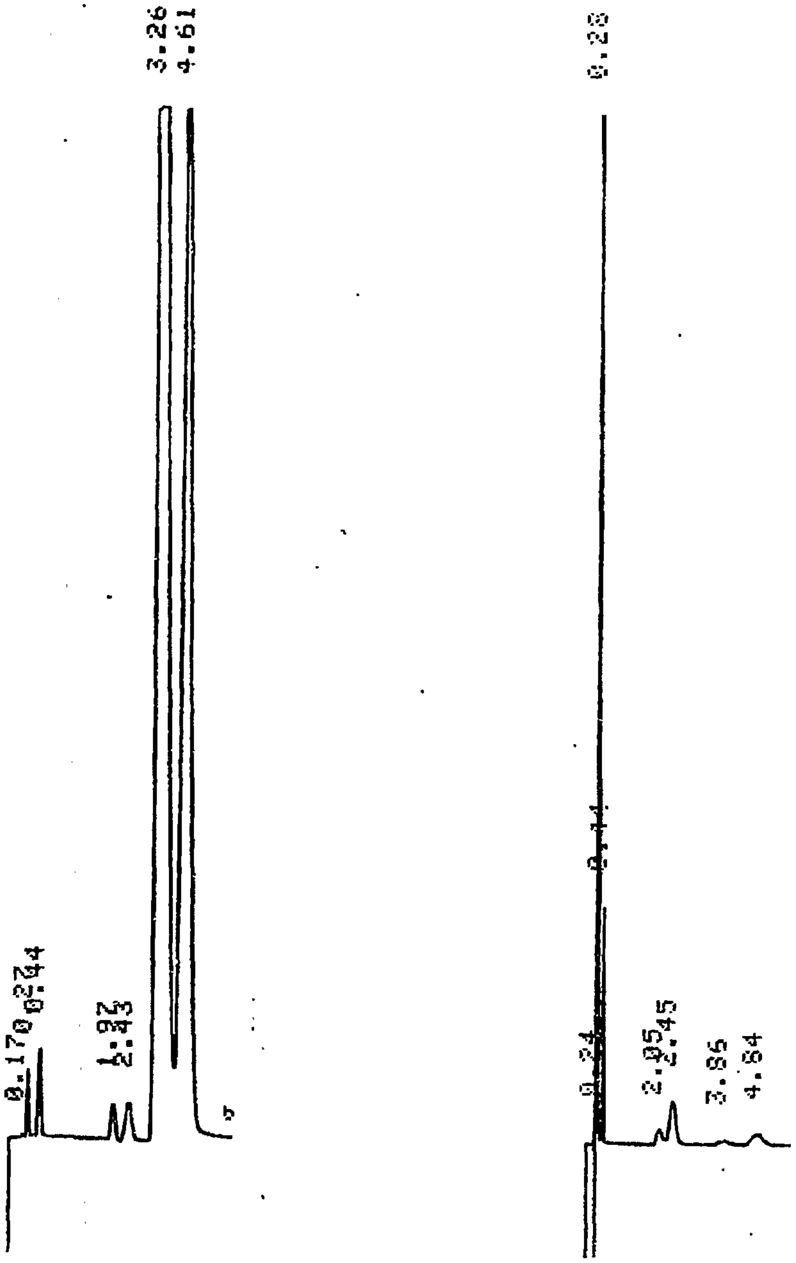

Liquid

Gas

Figure 3. Gas Chromatogram of Typical Gas and Liquid Samples

reported that the three by-products were CO_2 (retention time of 0.44), H_2O (retention time from 1.85 to 2.05) and DME (retention time from 2.30 to 2.43).

1.7 Modeling of Non-Isothermal Fischer-Tropsch Slurry Reactors

During the last quarter Dr. Yatish T. Shah left the University of Pittsburgh and became Dean of Engineering and Science at the University of Tulsa. He was replaced as Principal Investigator by John W. Tierney. However, he is continuing to particpate in the project as a consultant. He is developing models of the Fischer-Tropsch process in a slurry reactor to serve as a guide to the experimental work which will be carried out and to aid in the analysis of the data. The status of this work to date is summarized in the following progress report.

Progress Report

September 1987

"Modeling of Non-Isothermal F-T Slurry Reactors"

Y. T. Shah
University of Tulsa
Tulsa, Oklahoma 74104

Submitted to
Professor Jack W. Tierney
Department of Chemical and Petroleum Engineering
University of Pittsburgh
Pittsburgh, PA 15261

INTRODUCTION

In recent years, there has been considerable interest in the use of slurry reactors for the Fischer-Tropsch (F-T) synthesis. [Deckwer et al (1980), Stern et al (1983), Bukur and Brown (1987)]. The purpose of this progress report is to present a model for non-isothermal unsteady state F-T slurry reactor.

The subject of non-isothermal slurry reactor has been reviewed in detail by Bhattacharjee and Shah (1984). A number of studies have been reported on the mathematical modeling of such reactors. Most of these studies have considered the case where a single reaction is assumed to occur in the reactor. It is also well known that in gas-liquid reactors in which a single irreversible exothermic reaction is carried out can exhibit up to five steady states [Hoffman et al (1975), Raghuram and Shah (1977)]. More general and interesting case of multiple reactions has not been investigated until the recent work by Bukur and Zimmerman (1987), who evaluated the performance of an isothermal bubble column slurry reactor for the multiple reactions.

It is clear from the available literature that a comprehensive modeling of F-T synthesis has to account for thermal effects as well as for the coupling between the F-T reaction and the water gas shift reaction which occurs in the reactor. The coupling of this phenomena has never been addressed before in the available literature. It is also pertinent to study the behavior of non-isothermal F-T synthesis, which as shown by Karandikar et al (1986), involves the effects of water on the solubilities and mass transfer coefficients for CO and H_2 in F-T liquids.

SYNTHESIS REACTIONS

Recent studies of the synthesis reaction on supported ruthenium catalyst [Dalla Betta et al (1979), Vannice (1975), Ekerdt and Bell (1979), Dixit and Tavlarides (1983), Bell and Heinemann (1983)] have indicated that products are mainly straight-chain hydrocarbons and predominantly methane under all reaction conditions. The formation of straight-chain hydrocarbons can be represented as:

$$nCO + (2n - 1)\ H_2 = C_n\ H_{2n+2} + nH_2O \qquad \text{(F-T)}$$

The shift reaction, which is thermodynamically favorable at typical synthesis reactions conditions is:

$$CO + H_2O = CO_2 + H_2 \qquad \text{(WGS)}$$

The shift reaction is mildly exothermic (40.9 kj/mol (at 298K), while the synthesis reaction is highly exothermic.

Different rate equations have been published in the literature, differing in the assumption of the rate-controlling step and corresponding dependence of rate equations in partial pressures of hydrogen and carbon monoxide [Stern et al.(1985)]. In the present study, various reliable expressions will be evaluated, and their influence in the final result will be compared.

The question of multiplicity of steady states arises because of the interaction between the rate of chemical reaction, the mass transport resistances and the solubility. The last two sets of variables are strongly coupled to the first one, in the light of the work by Karandikar et al (1986). The dissolved water (due to the water gas shift reaction) shows a synergistic effect and minimizes the foaming tendency of the F-T liquid. The solubilities of CO and H_2 markedly increase with the presence of water and the effect being more pronounced for H_2 than for CO. Mass transfer coefficient for H_2 decreases and that for CO increases due to the presence of water. These effects are clearly shown in Figures 1-4 (from Karandikar et al. (1986)).

MATHEMATICAL MODELING

The following equations represent the mass balances for CO, H_2 and H_2O as well as the heat balance for the three-phase F-T synthesis reactor.

In the development of the equations, it is assumed that the system is adiabatic, mass transfer resistances are only in the liquid phase and there is no temperature difference between the gas-liquid and solid phases. It is also assumed that both liquid and gas holdups are constant, and the reactions take place at the solid surface. The liquid phase is considered as a single phase, despite having some evidence of a two separate fractions: one rich in water and the other in hydrocarbons [Karandikar et al. (1986)].

GAS PHASE

Mass balance for CO:

$$V_G \frac{dC_{CO}}{dt} = F^G_{CO,f} - F^G_{CO} - K_{L_{CO}} (T, C^L_{H_2O}) \; a \; V_L \; x$$

$$(C^*_{CO} \; (T, C^L_{H_2O}) - C^L_{CO}) \qquad (1)$$

Mass balance for H_2:

$$V_G \frac{dC_{H_2}}{dt} = F^G_{H_2,f} - F^G_{H_2} - K_{L_{H_2}}(T, C^L_{H_2O})\, a\, V_L \times$$

$$(C^*_{H_2}(T, C^L_{H_2O}) - (C^L_{H_2})) \tag{2}$$

Mass balance for H_2O:

$$V_G \frac{dC_{H_2O}}{dt} = F^G_{H_2O,f} - F^G_{H_2O} + F_{ev} \tag{3}$$

where V_G = volume of the gas phase, it has been assumed constant, as well as it has been neglected any mass transfer resistance in the gas phase. C_i stands for molar concentration of ith species, t is time, $F^G_{i,f}$ is the molar feed rate in the gas phase of the ith species. F_i^G is the exit molar rate in the gas phase of the ith species. K_{L_i} is the liquid-gas mass transfer coefficient for the ith species, a is the specific gas liquid interfacial area, V_L is the volume of the liquid phase (assumed constant). C^*_i is the equilibrium concentration for the ith species. C_i is the exit concentration of the ith species in the gas phase. F_{ev} is the molar rate of water evaporation.

LIQUID PHASE

Mass balance for CO:

$$V_L \frac{dC^L_{CO}}{dt} = F^L_{CO,f} - F^L_{CO} + K_{L_{CO}}(T, C^L_{H_2O})\, a\, V_L\, (C^*_{CO}(T, C^L_{H_2O}) - C^L_{CO})$$

$$- K_{S_{CO}}\, a_p\, V_L\, (C^L_{CO} - C^S_{CO}) \tag{4}$$

Mass balance for H_2:

$$V_L \frac{dC_{H_2}}{dt} = F^L_{H_{2,f}} - F^L_{H_2} + K_{L_{H_2}} (T, C^L_{H_2O})\ a\ V_L\ (C^*_{H_2} (T, C^L_{H_2O}) - C^L_{H_2})$$

$$-K_{S_{H_2}}\ a_p\ V_L\ (C^L_{H_2} - C^S_{H_2}) \qquad (5)$$

Mass balance for H_2O:

$$V_L \frac{dC^L_{H_2O}}{dt} = F^L_{H_{2,f}} - F^L_{H_2O} - F_{ev} + K_{S_{H_2O}}\ a_p\ V_L\ (C^L_{H_2O} - C^S_{H_2O}) \qquad (6)$$

Where C^L_i is the molar concentration of the ith species in the liquid phase, K_{S_i} is the liquid solid mass transfer coefficient in the liquid phase for ith species. a_p is the liquid solid interfacial area. C^S_i is the concentration of the ith species at the solid surface.

SOLID PHASE

Mass balance for CO:

$$K_{S_{CO}}\ a_p\ V_L\ (C^L_{SO} - C^S_{SO}) = C_c\ V_L\ (-n r_{FT} - r_{WGS}) \qquad (7)$$

Mass balance for H_2:

$$K_{S_{H_2}}\ a_p\ V_L\ (C^L_{H_2} - C^S_{H_2}) = C_c\ V_L\ (-\ (2n+1)\ r_{FT} + r_{WGS}) \qquad (8)$$

Mass balance for H_2O:

$$K_{S_{H_2O}}\ a_p\ V_L\ (C^L_{H_2O} - C^S_{H_2O}) = C_c\ V_L\ (n\ r_{FT} - r_{WGS}) \qquad (9)$$

Where C_c is the concentration of catalyst in the liquid, r_{FT} is the rate of Fischer-Tropsch reaction, r_{WGS} is the rate of water gas shift reaction.

ENGERY BALANCE

$$[r_{FT}\ (-\ \Delta H_{FT}) + r_{WGS}\ (-\Delta H_{WGS})]\ V_L\ C_c + K_{L_{CO}}\ (T, C^L_{H_2O})\ a\ \times$$

$$(C^*_{CO}\ (T, C^L_{H_2O}) - C^L_{CO})\ (-\Delta H_{S_{CO}}) + K_{L_{H_2}}\ (T, C^L_{H_2O})\ a\ (C^*_{H_2}\ (T, C^L_{H_2O})\ \times$$

$$(-\Delta H_{S_{H_2}}) + (F^{SL}_f C^{SL}_p + F^G_f\ C^G_p)\ T_f - (F^{SL} C^{SL}_p + F^G\ C^G_p)\ T - F_{ev}\ \times$$

$$(-\Delta H_{ev}) = (M^{SL} C^{SL}_p + M^G\ C^G_p)\ \frac{dT}{dt} \qquad (10)$$

Where T is the temperature in the reactor, T_f is the feed temeperature, C_p are heat capacities, M^{SL} is the total number of moles in the slurry (liquid and solid) and M^G in the gas phase. F^{SL} and F^G are the total mole rates in each phase. $-(\Delta H)_i$'s are heat of reaction, $(-\Delta H)_{ev}$ is heat of evaporation, and $(-\Delta H)_s$ is heat of dissolution.

MULTIPLE STEADY-STATES

The analysis for multiple steady-states considers the solution of equations (1)-(10), neglecting the transient terms of each of them (the complete system can be used for stability analysis).

When the heat generated by the system [the first three terms in equation (10)] and the heat removed from the system [the last three terms in LHS of equation (10)] are drawn as a function of the temperature, every intersection between these two graphs represents a steady state solution. For determining those curves, the concentrations of every species in the three phases have to be calculated. Then, the algebraic problem becomes three phases have to be calculated. Then, the algebraic problem becomes non-linear, because of the functionality of solubilities, mass transfer coefficients and kinetic constants on temperature, and water content (see Figures 1-4). [Deimling et al (1984), Karandikar et al (1986)]. It can be anticipated, that for the solution of the algebraic system an iterative method of solution has to be implemented, using some Newton-Raphson subroutine.

As it has already been mentioned, there is enough information about mass transport properties of the system in the literature. Nevertheless, the complete adiabatic problem solution is not trivial; in particular, multiple steady-states for a highly coupled system of multiple reactions as this is, presents features not addressed previously in literature, and especially in Fischer-Tropsch synthesis.

SEMI-BATCH OPERATION

It can be also considered, as a particular case, the operation of the slurry reactor with the slurry phase (liquid plus solid) as a stationary phase. In this case, it is necessary to retain the transient terms in equations (1 - 10), because the volume of the phases will vary with time (that assumption has to be removed).

The equation for this kind of operation are as follows:

GAS PHASE

Mass balance for CO:

$$C_{CO}\frac{dV_G}{dt} + V_G\frac{dC_{CO}}{dt} = F^G_{CO,F} - F^G_{CO} - K_{L_{CO}}(T,C_{H_2O})\, a\, V_L \times$$

$$(C^*_{CO}(T,C^L_{H_2O}) - C^L_{CO}) \qquad (11)$$

Mass balance for H_2:

$$C_{H_2}\frac{dV_G}{dt} + V_G\frac{dC_{H_2}}{dt} = F^G_{H_{2,f}} - F^G_{H_2} - K_{L_{H_2}}(T,C^L_{H_2O})\ a\ V_L\ \times$$

$$(C^*_{H_2}(T,C^L_{H_2O}) - C^L_{H_2}) \qquad (12)$$

Mass balance for H_2O:

$$C_{H_2O}\frac{dV_G}{dt} + V_G\frac{dC_{H_2O}}{dt} = F^G_{H_{2,f}} - F^G_{H_2O} + F_{ev} \qquad (13)$$

where nomenclature is as in the previous part.

LIQUID PHASE

Mass balance for CO:

$$C^L_{CO}\frac{dV_L}{dt} + V_L\frac{dC^L_{CO}}{dt} = K_{L_{CO}}(T,C^L_{H_2O})\ a\ V_L\ (C^*_{CO}(T,C^L_{H_2O}) - (C^L_{CO}))-$$

$$K_{S_{CO}}\ a_p\ V_L\ (C^L_{CO} - C^S_{CO}) \qquad (14)$$

Mass balance for H_2:

$$C^L_{H_2}\frac{dV_L}{dt} + V_L\frac{dC^L_{H_2}}{dt} = K_{L_{H_2}}(T,C^L_{H_2})\ a\ V_L(C^*_{H_2}(T,C^L_{H_2O}) - C^L_{H_2})-$$

$$K_{S_{H_2}}\ a_p\ V_L\ (C^L_{H_2} - C^L_{H_2}) \qquad (15)$$

Mass balance for H_2O:

$$C^L_{H_2O} \frac{dV_L}{dt} + V_L \frac{dC^L_{H_2O}}{dt} = -F_{ev} + K_{S_{H_2O}} a_p V_L (C^L_{H_2O} - C^S_{H_2O}) \qquad (16)$$

SOLID PHASE

Mass balance for CO:

$$K_{S_{CO}} a_p V_L (C^L_{S_O} - C^S_{S_O}) = C_c V_L (-nr_{FT} - r_{FT}) \qquad (17$$

Mass balance for H_2O:

$$K_{S_{H_2}} a_p V_L (C^L_{H_2O} - C^S_{H_2}) = C_c V_L (-(2n+1) r_{FT} + r_{WGS}) \qquad (18)$$

Mass balance for H_2O:

$$K_{S_{H_2O}} a_p V_L (C^L_{H_2O} - C^S_{H_2O}) = C_c V_L (nr_{FT} - r_{WGS}) \qquad (19)$$

ENERGY BALANCE

$$[r_{FT}(-\Delta H_{WGS})] V_L C_c + K_{L_{CO}} (T, C^L_{H_2O}) a (C^*_{CO}(T, C^L_{H_2O}) - C^L_{CO}) \times$$

$$(-\Delta H_{S_{CO}}) + K_{L_{H_2}} (T, C^L_{H_2O}) a (C^*_{H_2O}(T, C^L_{H_2O}) - C_{H_2}) (-\Delta H_{S_{H_2}}) +$$

$$F_f^G C_p^G T_f - F^G C_p^G T - F_{ev} (-\Delta H_{ev}) =$$

$$(M^{SL} C_p^{SL} + M^G C_p^G) \frac{dT}{dt} + C_p^{SL} T \frac{dM^{SL}}{dt} + C_p^G T \frac{dM^G}{dt} \qquad (20)$$

Also,

$$\frac{dV_G}{dt} = - \frac{dV_L}{dt} \quad \text{and} \quad \frac{dM^L}{dt} = - \frac{dM^G}{dt} \qquad (21)$$

The initial conditions for Eqs. (11) - (20) are:

$V_L = V_G^{o}$ initial gas volume

$C_{CO} = C_{CO}^{o}$ initial concentration of CO in the gas phase.

$C_{H_2} = C_{H_2}^{o}$ initial concentration of H2 in the gas phase.

$C_{H_2O} = C_{H_2O}^{o}$ initial concentration of H_2O in the gas phase.

$C_{CO}^{L} = C_{CO}^{L\,o}$ initial concentration of CO in the liquid phase.

$C_{H_2}^{L} = C_{H_2}^{L\,o}$ initial concentration of H2 in the liquid phase.

$C_{H_2O}^{L} = C_{H_2O}^{L\,o}$ initial concentration of H_2O in the liquid phase.

$T = T^{o}$ initial temperature of the liquid (assumed to be the same as the gas temperature).

$M^{L} = M^{Lo}$ initial number of moles in the liquid phase.

$M^{G} = M^{Go}$ initial number of moles in the gas phase.

$M^{SL} = M^{SLO}$ initial number of moles in the slurry phase

NOMENCLATURE

a, a_p	specific interfacial area
C	concentration
C^*	solubility
F	flowrate
K	mass transfer coefficient
M	molal flowrate
n	alpha number for F-T reaction
r	rate of reaction
t	time
T	temperature
V_G, V_L	gas and liquid velocities
ΔH_r	heat of reaction
ΔH_S	heat of solution

Subscripts

f	feed
G	gas
L	liquid
CO, H_2, H_2O	pertain to species

Superscripts

G	gas
L	liquid
SL	slurry

REFERENCES

Bhattacharjee, S. and Shah, Y.T., in "Recent Advances in the Engineering Analysis of Chemically Reacting Systems", ed. by L. K. Doraiswamy, Wiley Eastern Pub. Co., New York (1984).

Bell, A.T.; Heinemann, H.; DOE report Oct. 1, 1983 - Dec. 31, 1983, Grant DE-FG22-81PC40795.

Bukur, D.B. and Brown, R.F. (to be published), (1986).

Bukur, D.B. and Zimmerman, W.H.; AIChE J., 33, 1197 (1987).

Dalla Betta, R.A., Piken, A.G. and Shelep, M.J.; J. Catal., 35, 54 (1974).

Deckwer, W.D.; Louisi, Y.; Zuidi, A. and Ralck, M.; Ind. Eng. Chem. Process Des. Dev., 19, 699 (1980).

Deimling, A.; Karandikar, B.M.; Shah, Y.T. and Carr, N.L.; Chem. Eng. J., 29, 127 (1984).

Dixit, R.J.; Tavlarides, L.L.; Ind. Eng. Chem. Process Des. Dev., 22, 1 (1983).

Ekerdt, J.G.; Bell, A.T.; J. Catal. 58, 170 (1979).

Hoffman, L.A.; Sharma, J.; Luss, D.; AIChE J., 21, 318 (1975).

Karandikar, B.M.; Morsi, B.I.; Shah, Y.T.; Carr, N.L.; Chem. Eng. J., 33, 157 (1986).

Raghuram, S.; Shah Y.T.; Chem. Eng. J., 13, 81 (1977).

Stern, D.; Bell, A.T.; Heinemann, H.; Chem. Eng. Sci., 38, 597 (1983).

Stern, D.; Bell, A. T.; Heinemann, H.; Chem. Eng. Sci., 40, 1665 (1985).

Vannice, M.A.; J. Catal., 37, 449 (1975).

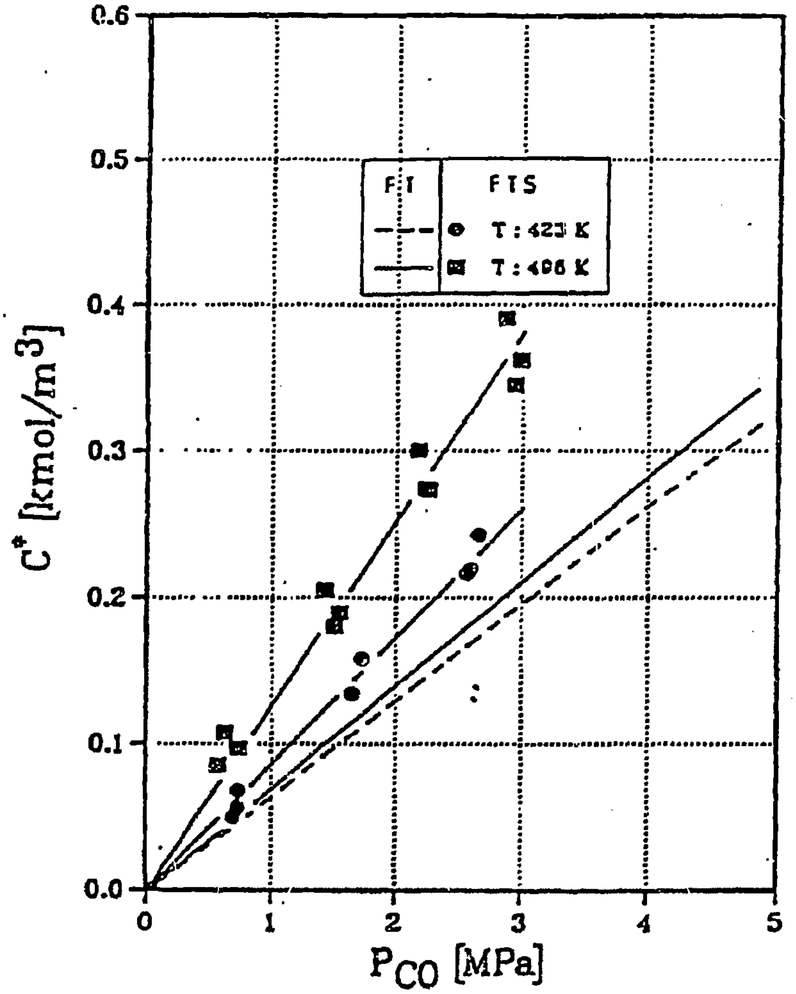

<u>Figure 1:</u> C^*_{co} vs. P_{co}

P_{CO} = partial pressure of CO (MPa).
C^*_{CO} = equilibrium CO Solubility (kmol/m^3)
FT = Fischer-Tropsch liquid
FTS = Fischer-Tropsch liquid saturated with water.

[From Karandikar et al (1986)]

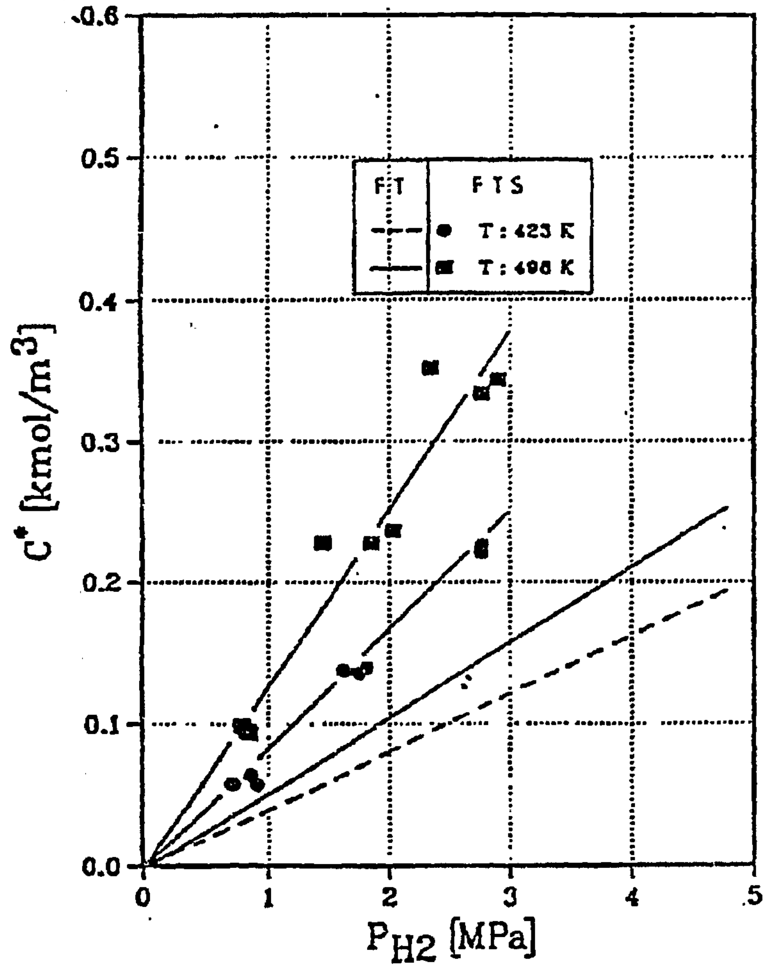

Figure 2: $C^*_{H_2}$ vs. P_{H_2}

P_{H_2} = partial pressure of H_2 (MPa).
$C^*_{H_2}$ = equilibrium H_2 Solubility (kmol/m^3).
FT = Fischer-Tropsch liquid
FTS = Fischer-Tropsch liquid saturated with water.

[From Karandikar et al (1986)]

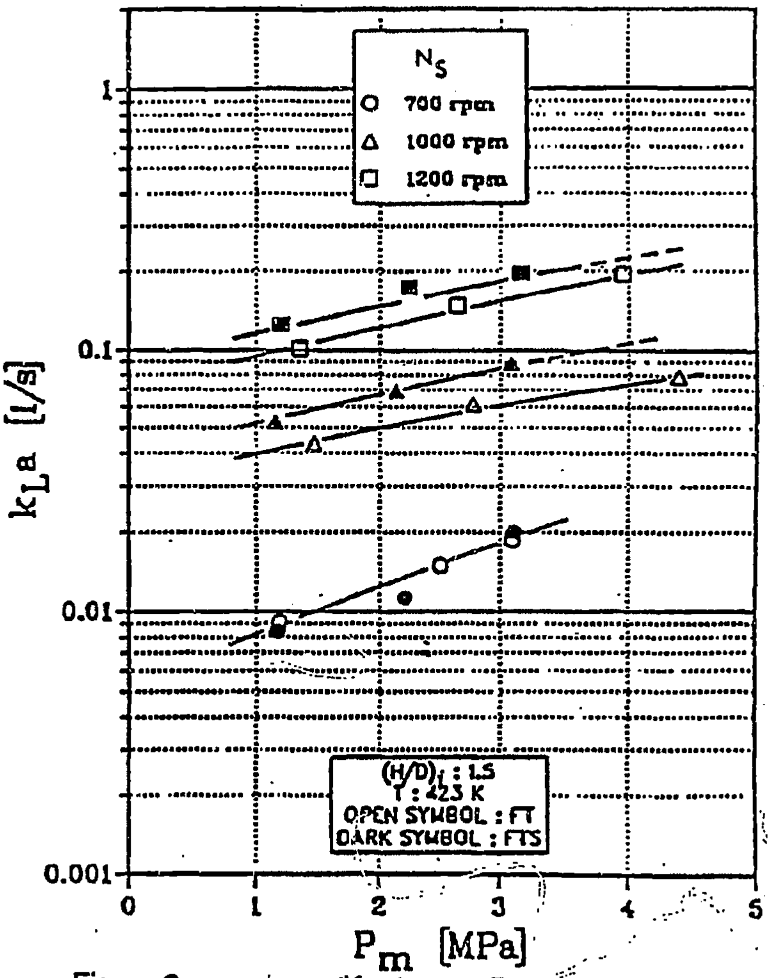

Figure 3: $(K_L\ a)_{co}$ vs. P_m

P_m = total mean pressure of CO (MPa).
$(K_L \cdot a)_{co}$ = mass transfer coefficient for CO (1/s).
N_S = stirrer speed (rpm).
$(H/D)_f$ = value of the ratio of the depth of the liquid to the diameter of the reactor, at the end of run.
FT = Fischer-Tropsch liquid.
FTS = Fischer-Tropsch liquid saturated with water.

[From Karandikar et al (1986)]

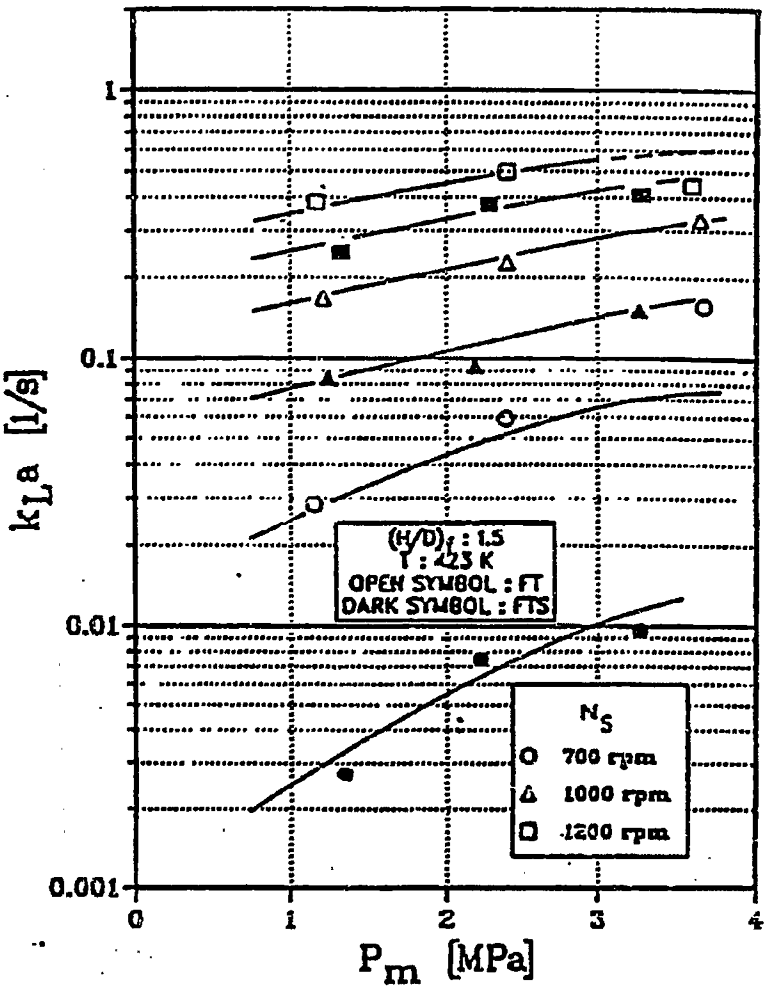

Figure 4: $(k_L a)_{H_2}$ vs. P_m

P_m = total mean pressure of H_2 (MPa).
$(K_L a)_{H_2}$ = mass transfer coefficient for H_2 (1/s).
N_S = stirrer speed (rpm).
$(H/D)_f$ = value of the ratio of the depth of the liquid to the diameter of the reactor, at the end of run.
FT = Fischer-Tropsch liquid.
FTS = Fischer-Tropsch liquid saturated with water.

[From Karandikar et al (1986)]

TASK 2: COAL LIQUEFACTION UNDER SUPERCRITICAL CONDITIONS

Supercritical fluid extraction is an attractive process primarily because the density and solvent power of a fluid changes dramatically with pressure at near critical conditions, and during the extraction of coal, the density of a supercritical fluid should also change the extractability of the coal. During earlier quarters a non-reacting supercritical fluid, toluene, was studied to determine the effect of density on the coal extraction/reaction process. Extractions were carried out for 2 to 60 minutes at reduced densities between 0.5 and 2.0 and at temperatures between 647 and 698 K. The data obtained can be explained by the hypothesis that coal dissolution is required preceding liquefaction reactions and that the degree of dissolution depends upon solvent density and temperature. A kinetic model shows that higher solvent densities result in faster conversion rates and in higher total conversions. Two papers have resulted from this study.

A second factor that makes supercritical extraction attractive is high mass transfer rates. At high pressures, mass transfer rates in a supercritical fluid are much higher than in a liquid, despite the fact that the supercritical fluid has liquid-like solvent powers. The objective of this work is to measure mass transfer rates for naphthalene extraction by carbon dioxide to enable us to determine how mass transfer coefficients vary with pressure, flow rate, and bed height, since these parameters will influence the design of extraction or reaction processes which utilize supercritical fluids. Ultimately, such measurements will be extended to coal/supercritical fluid systems to help define the flow rates liquid/solvent ratios that would be appropriate for a supercritical system.

In this report, the entire program for evaluating mass transfer coefficients under supercritical conditions is described and a review of current knowledge and planned correlational approaches is given.

2.1 Background

Historically, interest in supercritical fluids was initially related to the observation that such fluids were often excellent solvents. This fact was discovered over 100 years ago by Hannay[12] and by Hannay and Hogarth.[13,14] Prior to that time, it was generally thought that materials above their critical temperatures would be gaseous in nature and thus poor solvents.

Studies of solubilities in supercritical fluids have been continued[15,16] and in most instances, they concentrated on developing phase diagrams for binary mixtures, particularly pressure-temperature projections. Vapor-liquid equilibrium data on binary hydrocarbon systems at elevated pressure became available in the 1930's[17,18] and the first patent for the practical application of supercritical extraction was made in 1943.[19] Later, Maddacks,[20] Tugrul[21] and Bartle et al.[22] described the extraction of components of low volatility from coal liquids using supercritical toluene. Barton and Fenske[23] suggested using C_{11} and C_{12} paraffinic fractions to desalinate sea water. Hubert and Vitzhu[24] studied on the removal of nicotine from tobacco leaves, of caffeine from green coffee beans, and the separation of a hop extract from commercial hops, in all cases using supercritical carbon dixoide. Modell et al.[25,26] discussed the regeneration of activated carbon by the use of supercritical carbon dioxide.

Critical data for a number of possible supercritical fluid solvents are listed in Table 2-1. These gases are suitable as a solvent either on their own or as components of mixtures. Because of their low critical temperatures, several of them can be used to extract heat-labile substances. Particularly, supercritical carbon dioxide is a very attractive solvent for practical applications because it is nonflammable, nontoxic, environmentally acceptable and relatively inexpensive. The critical temperature of carbon dioxide is only 304°K (31°C) and thus it can be used at moderate temperature for the extraction of heat sensitive substances without degradation. One good example of using supercritical carbon dioxide is shown in selective extraction of caffeine from green coffee beans.

Table 2-1: Critical Data for Some Supercritical Solvents[79]

Substance	Critical Temperature K	Critical Pressure MPa	Critical Density g cm^{-1}
Methane	191	4.60	0.162
Ethylene	282	5.03	0.218
Chlorotrifluoro methane	302	3.92	0.579
Carbon dioxide	304	7.38	0.468
Ethane	305	4.88	0.203
Propylene	365	4.62	0.233
Propane	370	4.24	0.217
Ammonia	406	11.3	0.235
Diethyl ether	467	3.64	0.265
n. Pentane	470	3.37	0.237
Acetone	508	4.70	0.278
Methanol	513	8.09	0.272
Benzene	562	4.89	0.302
Toluene	592	4.11	0.292
Pyridine	620	5.63	0.312
Water	647	22.0	0.322

The supercritical fluid (SCF) region is not defined rigorously, but for the practical considerations, the SCF region is usually defined at conditions bounded approximately by $0.9 < T_r < 1.2$ and $P_r > 1.0$ where the SCF is very compressible as illustrated in Figure 2-1. For example, at a constant T_r of 1.0, increasing pressure from $P_r = 0.8$ to $P_r = 1.2$ significantly increases the density from gas-like densities to liquid-like densities. At higher reduced temperature, the pressure increase required to increase an equivalent density becomes greater. This practical consideration sets the upper bound on temperature. At higher pressures, the density is less sensitive to temperature changes. In the vicinity of the critical

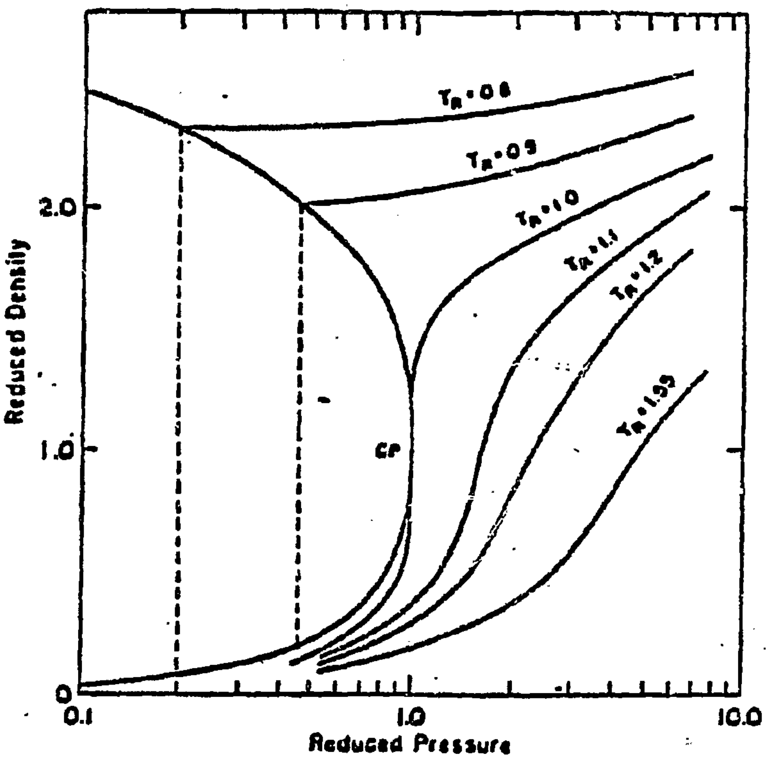

Figure 2-1: Reduced density–reduced pressure diagram for carbon dioxide at various reduced temperatures[35] (T_r) in the vicinity of the critical point(CP)

point, large density changes can be obtained with either relatively small pressure or temperature changes.

The effect of SCF solvent density on solubilities is shown directly in Figure 2-2 in the naphthalene-ethylene system.[27,28] Solubilities increase with increasing ethylene densities along each isotherm due to increasing solvent power, and with increasing temperature at constant density due to increasing volatility of naphthalene. These solvent properties vary continuously with solvent density and thus control solvent power and enhance the selectivity of the solvent. Also solvent and solute can be easily separated, and we can fractionate multiple solutes by stepwise reductions in solvent density.

In addition, SCF have better physicochemical properties than do gases and liquids. The order-of-magnitude comparison shown in Table 2-2 indicates that, while SCF has liquid-like densities, its viscosities and diffusivities are intermediate to those properties for liquids and gases. Thus SCF has the solvent power of liquids with better mass-transfer properties.

Table 2-2: Order of Magnitude Comparison of Gas, SCF and Liquid Phases[35]

		Phase	
Property	Gas	SCF*	Liquid
Density (kg/m^3)	1	700	1000
Viscosity (Ns/M^2)	10^{-5}	10^{-4}	10^{-3}
Diffusion coefficient (cm^2/s)	10^{-1}	10^{-4}	10^{-5}

---

* At $T_r = 1$ and $P_r = 2$

** 10^3 centipoise = 1 Ns/m^2

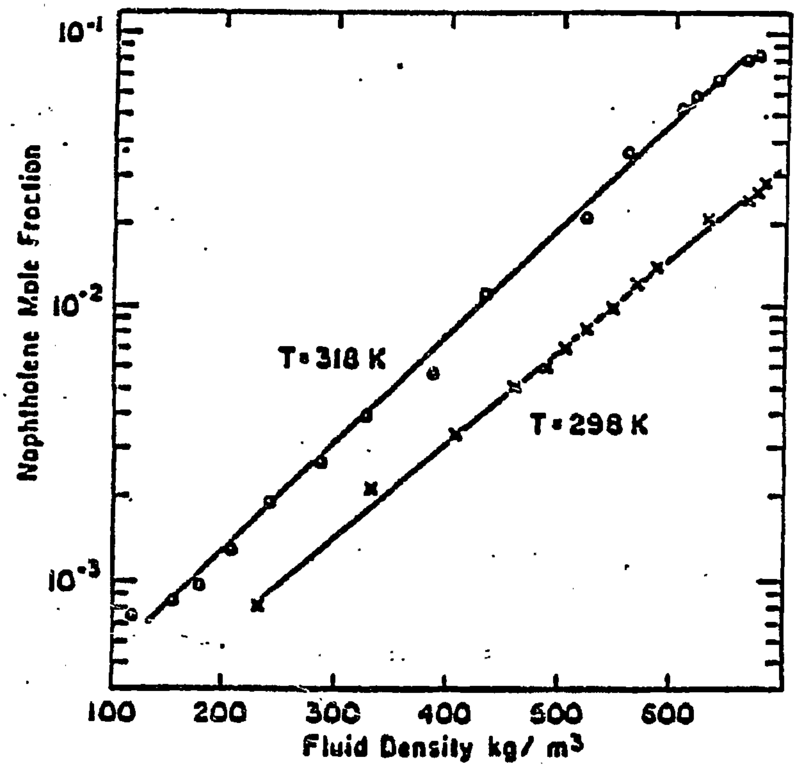

Figure 2-2: Solid solubilities of naphthalene in compressed ethylene as a function of ethylene density

2.2 Diffusion Coefficient and Viscosity

The development of mass-transfer models requires knowledge of the diffusion coefficient of the solute, the viscosity, and the density of the fluid phase which can be used to correlate mass transfer coefficients.

Experimental data on diffusion coefficients in supercritical condition are scarce. Most studies on diffusion coefficient in the high pressure had been limited to the measurement of self diffusion coefficients, and binary diffusion coefficients in simple systems such as H_2-N_2, He-N_2 and H_2-Ar.[32] But recently, several experiments has been done to measure the diffusivities in systems such as naphthalene-CO_2,[33,34] benzene-CO_2 and caffeine-CO_2.[33] As a result of this work, it has been found that the viscosities and diffusivities of supercritical fluids were strongly dependent upon pressure and temperature in the vicinity of the critical point, and the ratios $(D_v\rho)/(D_v\rho)^o$ were 0.8 to 1.2. $(D_v\rho)^o$ is the value calculated on the basis of the low density theory for a gas at the given temperature. In the recent review article,[35] diffusion coefficient for the several systems were shown as a function of reduced pressure in Figure 2-3.

The viscosity of compressed fluids have been studied quite extensively. In Figure 2-4, the typical data of the viscosities of supercritical carbon dioxide is given as a function of pressure.[36] At the low pressure, the viscosities of carbon dioxide are essentially independent of pressure, but above the critical pressure, the viscosities increase rapidly with pressure.

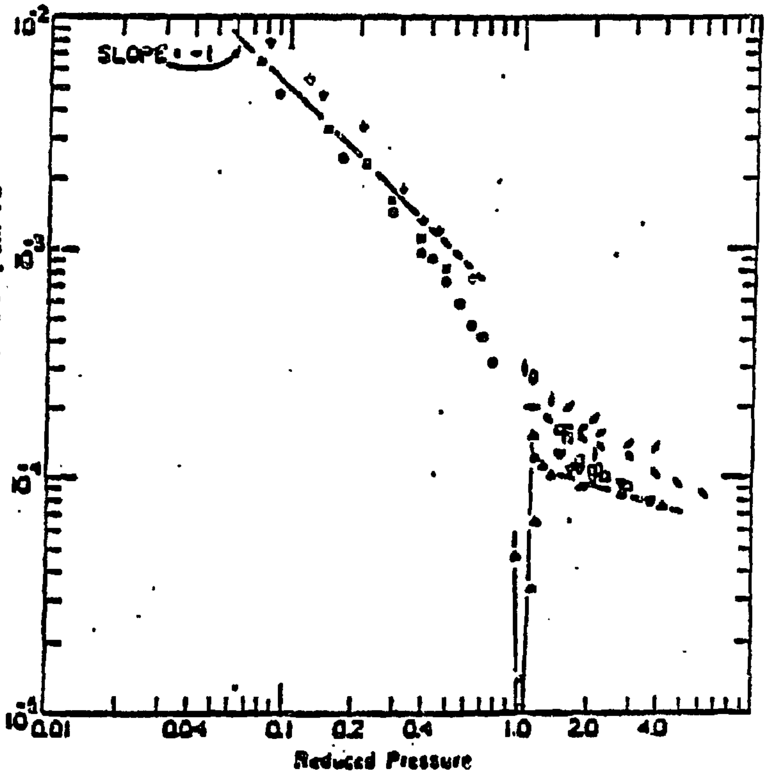

Figure 2-3: Diffusion coefficient in supercritical fluids[35]

Table 2-3: Key for figure 2-3.

Symbol	T, °C	System	Reference
•	20	CO_2-Naphthalene	56, 57
x	30		
+	40		
△	35	CO_2-Naphthalene	58
▽	55		
—	12	Ethylene-Naphthalene	58
/	35		
¦	40	CO_2-Benzene	60
—•—	40	CO_2-Propylbenzene	34
◇	40	CO_2-1,2,3-Trimethylbenzene	34

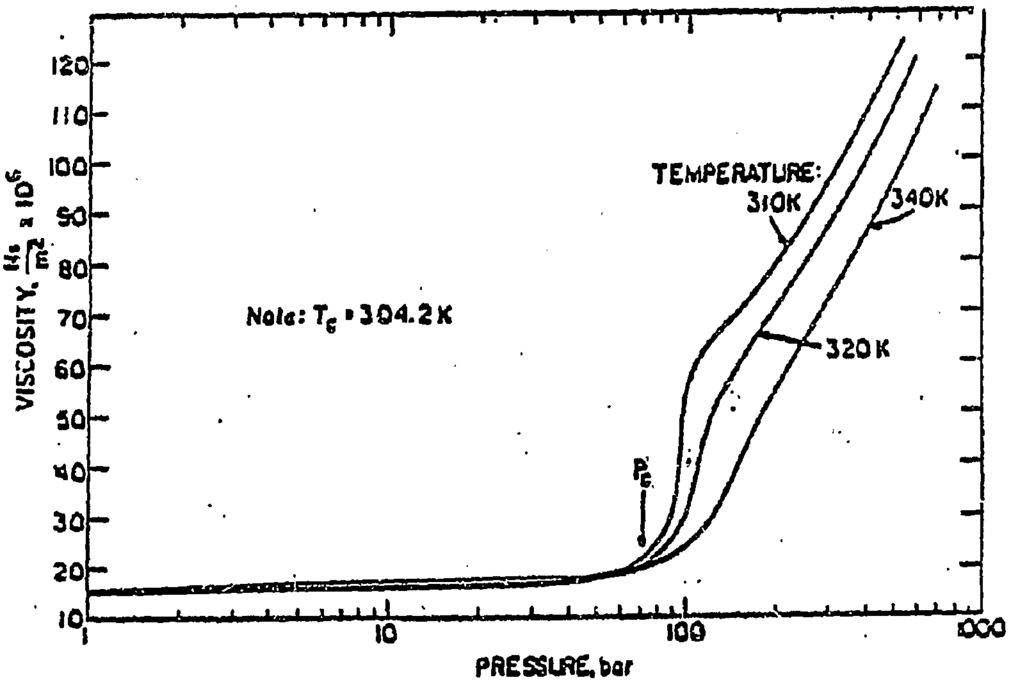

Figure 2-4: Viscosity of supercritical carbon dioxide[35]

2.3 Models for Flow System in a Packed Bed

The packed bed reactor is applicable in many operations, such as extraction, adsorption, leaching, ion exchange and catalytic processes. Therefore, mass-transfer coefficients in packed beds is the focus of the current research. First models for determining mass transfer from our experiments (past 38) will be developed and then these coefficients will be correlated.

The simplest flow model for the packed bed is the ideal plug flow model with no longitudinal mixing but complete radial mixing. Although no actual reactors can be fully represented by an ideal model, the plug flow model can be used in a number of packed bed reactors which behave close to the ideal.

However, flow behavior of most of the actual packed bed reactors deviates from ideal conditions. The deviation may be caused by nonuniform velocity profile, velocity fluctuation due to molecular or turbulent diffusion, by short-circuiting, by-passing and channeling of fluid, and by the presence of stagnant regions of fluid caused by the reactor shape and internals. Many flow models considering the nonideality of the flow pattern in packed reactor have been proposed.[37-41] Among them, the cell model or compartment model[40,41] is one of the most widely used models owing to its advantages over other models as decribed below. We used these two models (ideal plug flow model and cell model) to get mass-transfer coefficients and estimate nonideality.

The Ideal Plug Flow Model

Flow patterns in packed bed reactors with small ratios of the tube and particle diameter to length can be closely approximated by plug flow. The measurement of mass-transfer coefficients is based upon the following equation:

$$dN_A = d(V_T y_A) = k_y(y_A^* - y_A)dA = k_y(y_A^* - y_A)a_S S dL \qquad (2\text{-}1)$$

Here,

$$V_T = \frac{1'}{1 - y_A} \qquad (2\text{-}2)$$

where V' is molal flow rate of inert component in moles per unit time. Therefore,

$$d(V_T y_A) = V'd\left(\frac{y_A}{1 - y_A}\right) = v' \frac{dy_A}{(1 - y_A)^2} = V_T \frac{dy_A}{(1 - y_A)} \qquad (2\text{-}3)$$

From equations (2-1) and (2-2)

$$\int_{y_{A,in}=0}^{y_{A,out}} \frac{dy_A}{(1 - y_A)(y_A^* - y_A)} = \frac{k_y a_S}{\bar{G}_{My}} \int_0^{L_T} dL \qquad (2\text{-}4)$$

where $\bar{G}_{My}$ is the average molal mass velocity of the gas in moles per unit area per unit time. For dilute gas (i.e., $1 - y_A \approx 1$),

$$\int_0^{y_{A,out}} \frac{dy_A}{y_A^* - y_A} = \left(\frac{k_y a_S}{\bar{G}_{My}}\right) L_T \qquad (2\text{-}5)$$

By integration and rearrangement,

$$k_y a_S = \left(\frac{\bar{G}_{My}}{L_T}\right) \ln \left(\frac{y_A^*}{y_A^* - y_{A,out}}\right)$$

Axial Dispersion in a Packed Bed

Several models have been used to analyze and correlate experimental data on mixing in a packed bed. They introduced radial and/or axial diffusion coefficients E_r and/or E_a, independent of solute concentration, to take into account the mixing effect in the radial and/or axial directions respectively, for packed beds. These diffusion coefficients can be realted to flow parameters, fluid properties and the geometry of the bed and the packing.

In a packed bed catalytic reactor, a chemical reaction takes place in a bed and heat flows through the tube wall and therefore, the radial heat and mass transfer are not negligible. However, radial dispersion can usually be neglected compared with axial dispersion when the ratio of column diameter to length is small and the flow is in the turbulent regime. Many investigators have found that the mixing effect in packed beds could be well described in an axial dispersion coefficient E_a alone even though there was some radial dispersion effect.

Dankwerts[41] first published the results on axial dispersion in a packed bed. Wen and Fan[42] summarized the results of previous investigations on the axial dispersion of liquids (Figure 2-5) and gases (Figure 2-6) in packed beds and have developed empirical correlations (shown below) based on about 500 data points for liquids and gases, respectively. The axial Peclet number $P_{e,a}$ is defined as $d_p u/E_a$. These equations can be used to determine the axial diffusion coefficient E_a for liquids and gases, respectively.

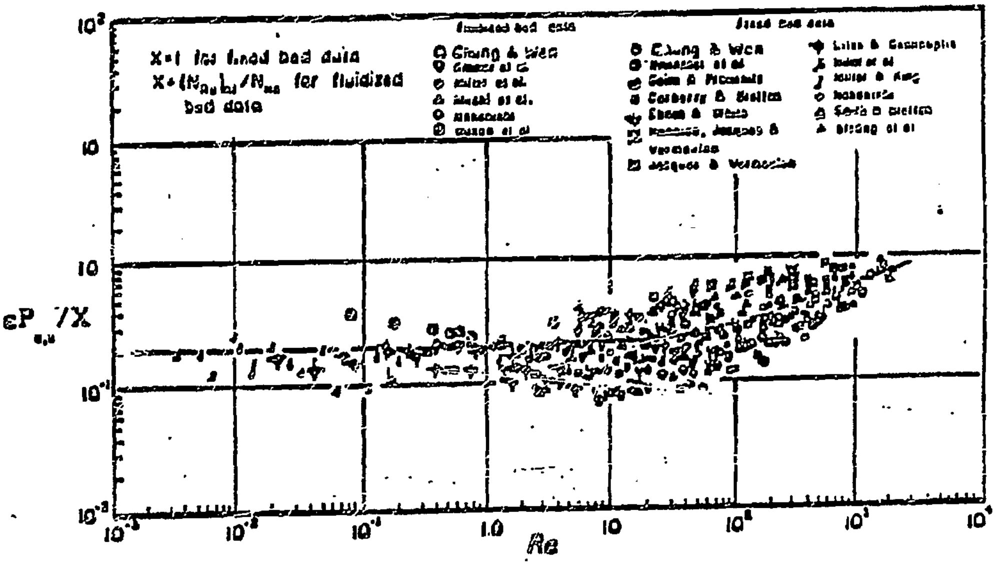

Figure 2-5: A Correlation of longitudinal dispersion coefficient of liquid phase fixed beds and fluidized beds in terms of peclet number[42]

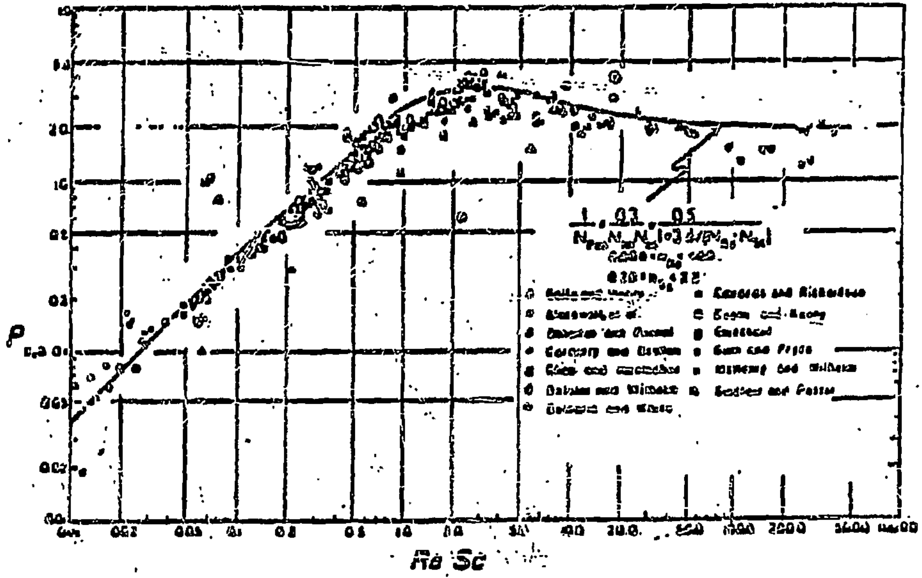

Figure 2-6: Correlation of axial dispersion coefficient for gases flowing through fixed beds[42]

Liquids:

$$\varepsilon P_{e,a} = 0.2 + 0.11\ \mathrm{Re}^{0.48} \tag{2-7}$$

Gases:

$$\frac{1}{P_{e,a}} = \frac{0.3}{\mathrm{ScRe}} + \frac{0.5}{1 + 3.8(\mathrm{ReSc})^{-1}} \tag{2-8}$$

for $0.008 < \mathrm{Re} < 400$ and $0.28 < \mathrm{Sc} < 2.2$

The general correlation of existing data of the axial dispersion coefficient for liquids and gases respectively[43] is shown in Figure 2-7. The dashed lines represent the molecular-diffusion asymptotes, for $Pe = (\mathrm{Re})(\mathrm{Sc})T_\varepsilon/\varepsilon$. The lines shown are for $T_\varepsilon = \sqrt{2}$ and $\varepsilon = 0.4$. In the case of gases, $P_{e,a}$ remains approximately constant,

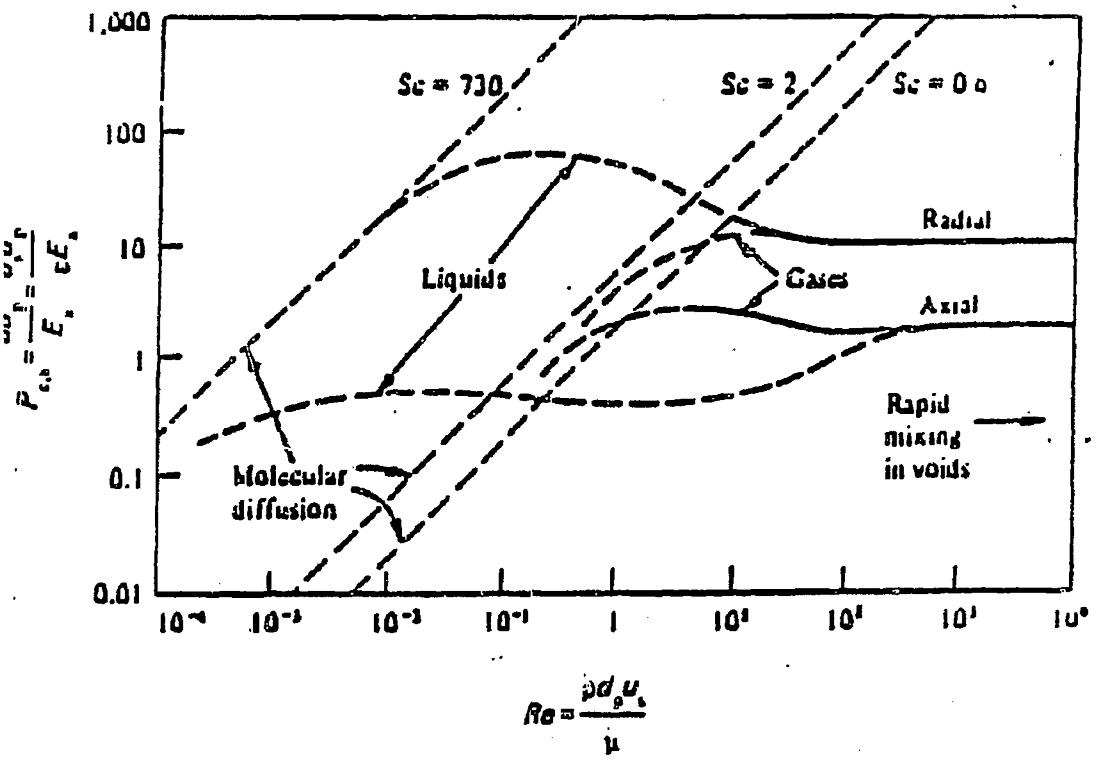

Figure 2-7: Approximate representation of a large amount of published data on radial and axial dispersion in randomly packed beds of uniform spheres: flow of a single phase[43]

decreasing little from its value of 2 until molecular diffusion is important at Re around 1.0. Molecular diffusion in liquids, however, is so slow that E_a increases as Re is reduced below 500. But as Re is decreased from 300 to 10, $P_{e,a}$ remains approximately proportional to Re indicating that E_a is roughly constant in this region. The correction of $P_{e,a}$ with Re is greatly dependent on the magnitude of the molecular diffusion coefficient D_v, that is, Schmidt number $Sc = \mu/\rho D_v$.

Even though no experimental data on axial dispersion have been published for supercritical fluids, we can approximate its effect as described below. For supercritical systems, the value of the Schmidt number, around 10, is intermediate to the values for gases ($Sc \approx 1.0$) and liquids ($Sc \approx 1000$). By comparing the order of magnitude of Schmidt number for gases, supercritical fluids and liquids, we can assume that the value of $P_{e,a}$ for SCF is so close to the value of $P_{e,a}$ for gas and is approximately equal to 2.0 when Re is greater than 1.0.

Kramers and Alberda[44] first discussed an analogy between a packed bed and a series of mixing vessels. By an analogy between the mechanism of imperfect mixing and Einstein's kinetic diffusion model, Carberry[37] showed that the number of perfect mixing tanks, n is given by:

$$n = \frac{Lu}{2E_a} = \frac{L}{d_p}\frac{P_{e,a}}{2} \qquad (2\text{-}9)$$

As $E_a \to \infty$ for n = 1.0, then for a small number of mixers less than 10:[44]

$$n - 1 = \frac{Lu}{2E_a} \qquad (2\text{-}10)$$

These equations are used for determining the number of perfect mixers to be used in the cell model below.

Mass-Transfer Coefficient from the Cell Model

The cell model is a generalization of a class of models such as the completely mixed tanks-in-series model and the back-flow mixed tanks-in-series model. The common characteristic of this model is that the basic mixing unit is a completely mixed or stirred tank. This model has been employed extensively from early days of chemical engineering to the present.[40,41,45-48] This cell model has the following practical advantages over other models:

1. The transition mixing behavior of such model can be presented by a set of linear first-order ordinary differential equations instead of partial differential equations.
2. The steady-state reaction in such a model can be represented by a set of finite difference equations rather than differential equations.

Since complete mixing is assumed in a cell, the mole fraction of a solute in out-going stream from the ith cell is y_i. If the bed is viewed as a series of n perfect mixing cells each having surface area of pellets A_T/n and constant mass-transfer coefficient k_y, then for the steady-state mass-transfer the material balance around the first cell gives

$$k_y(A_T/n)(y^* - y_1) = V_T(y_1 - y_0) \qquad (2\text{-}11)$$

Finally, we can obtain the following expression for n cells by using the similarity for each cell (its derivation is not given here)

$$k_y a_S = \frac{nV_T}{SL_T} \left[\left(\frac{y^* - y_0}{y^* - y_n} \right)^{1/n} - 1 \right] \qquad (2\text{-}12)$$

As mentioned above, we can assume that the value of $P_{e,a}$ for SCF is approximately equal to 2.0 when Re is greater than 1.0. Then, the number of perfect mixers in a packed bed can be determined by equation (2-9) or (2-10) depending upon the number of layers of the pellets in a packed bed (L/d_p). Finally, the mass-transfer coefficient under supercritical conditions can be obtained by equation (2-6) and/or (2-12) using the plug flow and/or cell models, respectively.

2.4 Mass-Transfer Correlations

After mass-transfer coefficients under supercritical conditions are determined, they need to be correlated as a function of the significant independent variables. Data on the rate of transfer between beds or particles and a flowing fluid are needed in the design of many industrial devices used for extraction, adsorption, leaching, ion exchange and chromatography. Numerous studies for packed beds have been carried out with the object of measuring mass-transfer coefficients and correlating the results under standard conditions, usually at 1 atm and 25°C. As far as we know, no data have been published on the mass-transfer coefficients under supercritical conditions. As several researchers pointed out,[10,11] under supercritical conditions we expect correlations for mass-transfer coefficients to differ from those for mass-transfer coefficients of solid-gas or solid-liquid systems under standard conditions.

In general, mass-transfer between a fluid and a packed bed of solid can be described by correlations of the following form by the similarity to the relationships obtained for heat transfer:

$$Sh = f(Re, Sc, Gr) \quad (2\text{-}13)$$

where Sh, Re, Sc, and Gr are respectively the Sherwood number, Reynolds, Schmidt, and Grashof numbers for the mass-transfer. Such a relationship has been obtained theoretically by Eckert[49] from a consideration of the boundary conditions.

Below we describe several existing correlations, developed under non-supercritical conditions, which may serve as guides for the correlations to be developed in this work.

Natural Convection

Recently, Debenedetti and Reid[50] pointed out that, in the case of supercritical fluids, buoyant effects had to be considered because supercritical fluids showed extremely small kinematic viscosities as a result of their high densitites and low viscosities. The comparison of the properties of air, water, and mercury was given in Figure 2-8 to show the relative importance of buoyant forces at constant Reynolds number. From the last column in Figure 2-8, we can find that the effect of buoyant forces is more than two orders of magnitude higher in supercritical fluid than in normal liquids.

For transfer under natural convection condition, where the Reynolds number is unimportant, general expression reduces to

$$Sh = g(Sc, Gr) \quad (2\text{-}14)$$

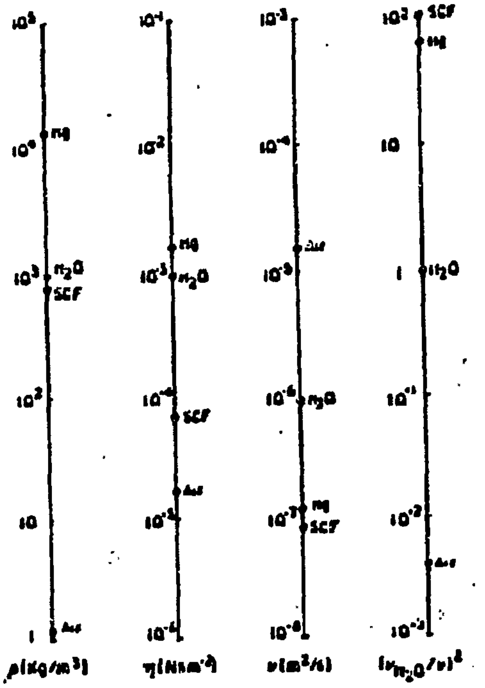

Figure 2-8: Comparison of physical properties of air, water, and mercury, and CO_2, showing relative importance of natural convection at constant Reynolds numbers; air, H_2O, Hg at 298°K and 1 bar, CO_2 at 310°K and 150 bar[50]

For large Schmidt number (usually liquid system) Karabeal et al.[51] proposed the following typical form of relationship for this natural convection condition by the use of asymptotic relations.

$$Sh = 0.46(GrSc)^{1/4} \qquad (2\text{-}15)$$

for laminar natural convection

$$Sh = 0.112(GrSc)^{1/3} \qquad (2\text{-}16)$$

for turbulent natural convection.

If natural convection is dominant, the correlations like those above are likely to be appropriate for modeling the mass-transfer coefficient data. Its main difference is that it is independent of Reynolds number Re.

Forced Convection

Under forced convection conditions, where the Grashof number is unimportant, the general expression becomes

$$Sh = h(Re,Sc) \qquad (2\text{-}17)$$

The most convenient method of correlating mass-transfer data under forced convection conditions is to plot the j_d factor as a function of Reynolds number as suggested by Colburn[5] and Chilton and Colburn[6] who, from theoretical consideration of flow and from dimensional analysis, defined j_d as follows:

$$j_d = \frac{Sh}{ReSc^{1/3}} = \frac{k_y M_{av}}{G}\left(\frac{\mu}{\rho D_v}\right)^{2/3} \qquad (2\text{-}18)$$

In calculating the Schmidt number, $\mu/\rho D_v$, the viscosity and density of carbon dioxide will be used since the amount of naphthalene in carbon dioixde has a negligible effect on these properties.

The functional dependence of j_d on Reynolds number Re has been the subject of study by many investigators. A variety of equations have been proposed to represent their experimental data. Many of these correlations also employ the bed porosity ε as an additional correlating parameter. The porosity is the ratio of the void volume between pellets to the total bed volume. Two typical correlations for solid-gas and solid-liquid systems are as follows:

1. Solid - Gas System:[52]

$$\varepsilon j_d = 0.357\ Re^{-0.359} \qquad 3 < Re < 2000 \qquad (2\text{-}19)$$

2. Solid-Liquid System:[8]

$$\varepsilon j_d = 0.25\ Re^{-0.31} \qquad 55 < Re < 1500 \qquad (2\text{-}20)$$

$$\varepsilon j_d = 1.09\ Re^{-2/3} \qquad 0.0016 < Re < 55 \qquad (2\text{-}21)$$

Other proposed correlations of mass-transfer data are shown in Rable 2-4.[51]

Combined Natural and Forced Convection

In the intermediate region where natural and forced convection happen simultaneously, neither the Reynolds number nor the Grashof number can be neglected. Garner and Grafton[53] suggested that the transfers due to the two processes are simply additive. Karabelas et al.[51] proposed the following correlations using an asymptotic method which are shown in Figure 2-9.

$$Sh = [\{0.46(GrSc)^{1/4}\}^6 + \{4.58\ pe^{1/3}\}^6]^{1/6} \qquad (2\text{-}22)$$

for 1 in, and 1/2 in, speheres ($GrSc < 1.31\text{x}10^8$)

$$Sh = [\{0.112(GrSc)^{1/3}\}^2 + \{2.39\ Re^{0.56}Sc^{1/3}\}^2]^{1/2} \qquad (2.23)$$

For 3 in, sphere ($GrSc = 3.2\text{x}10^9$)

Table 2-4: Correlations of mass-transfer data[51]

Reference	Type of packing	Correlation	Re	Sc
61	Spherical and cylindrical pellets	$j_d = 16{\cdot}8Re^{-1}$	< 40	0·61–0·62
		$j_d = 0{\cdot}989Re^{-0{\cdot}41}$	> 350	
62	Same as above	$j_d = 1{\cdot}82Re^{-0{\cdot}51}$	< 350	~ 0·615
63	Granular solid	$StSc^{0{\cdot}6} = 0{\cdot}45Re^{-0{\cdot}50}$	< 10	~ 1000
		$StSc^{0{\cdot}6} = 0{\cdot}20Re^{-0{\cdot}38}$	> 50	
64	Spheres and cylinders	$j_d = 1{\cdot}251Re_m^{-0{\cdot}41}$	$Re_m > 620$	~ 0·61
		$j_d = 2{\cdot}44Re_m^{-0{\cdot}51}$	$Re_m < 620$	
65	Spherical and flake shaped particles	$j_d = 1{\cdot}625Re^{-0{\cdot}507}$	< 120	1200–1500
		$j_d = 0{\cdot}687Re^{-0{\cdot}327}$	> 120	
66	Porous spherical particles soaked in an aqueous solution	$\log j_d = 0{\cdot}7683 - 0{\cdot}915\log Re + 0{\cdot}0817(\log Re)^2$	0–10,000	776 and 865
67	Pellets of succinic and salicylic acids	$StSc^{-0{\cdot}58} = 1{\cdot}97\left[\frac{Re}{\epsilon}\right]^{-0{\cdot}612}$	$\frac{Re}{\epsilon} < 200$	150–13,000
		$StSc^{-0{\cdot}58} = 0{\cdot}29\left[\frac{Re}{\epsilon}\right]^{-0{\cdot}384}$	$\frac{Re}{\epsilon} > 200$	
68	Various particle geometries	$j_d = \frac{150(1-\epsilon)}{6\epsilon}Re^{-1}Sc^{-1/3} + \frac{1{\cdot}75}{6\epsilon}Sc^{-1/3}$	wide range	wide range
69	Spheres	$j_d = 1{\cdot}46\left[\frac{6G}{a\mu}\right]^{-0{\cdot}41}(1-\epsilon)^{0{\cdot}2}$	$\frac{6G}{a\mu} > 100$	wide range
		$j_d = 17\left[\frac{6G}{a\mu}\right]^{-1}(1-\epsilon)^{0{\cdot}2}$	$\frac{6G}{a\mu} < 10$	
70	Porous spheres	$j_d = 10Re^{-1}$	< 30	low
		$j_d = 1{\cdot}30Re^{-0{\cdot}45}$	> 150	
71	Benzoic acid granules	$j_d = 1{\cdot}48Re^{-0{\cdot}52}$	1–70	~ 1000
72	Various particle types	$j_d = 5{\cdot}7\left[\frac{Re}{1-\epsilon}\right]^{-0{\cdot}78}$	$1 < \frac{Re}{1-\epsilon} < 30$	0·6–10,000
		$j_d = 1{\cdot}77\left[\frac{Re}{1-\epsilon}\right]^{-0{\cdot}44}$	$30 < \frac{Re}{1-\epsilon} < 10^4$	
73	Spherical particles	$j_d = 0{\cdot}667Re^{-0{\cdot}26}$	20–200	
74	Porous spheres	$j_d = \frac{0{\cdot}725}{Re^{0{\cdot}41} - 1{\cdot}5}$	13–2136	0·606
7	Fixed and fluidized beds of spheres	$\epsilon j_d = 0{\cdot}010 + \frac{0{\cdot}863}{Re^{0{\cdot}58} - 0{\cdot}483}$	> 1	wide range
75	Fixed and fluidized beds of particles with various geometries	$\frac{\epsilon j_d}{f} = \frac{0{\cdot}30}{Re_m^{0{\cdot}35} - 1{\cdot}90}$	$Re_m > 50$	wide range
76	Spherical particles	$StSc^{2/3} = 2{\cdot}40\left[\frac{Re}{\epsilon}\right]^{-0{\cdot}66}$	$0{\cdot}08 < \frac{Re}{\epsilon} < 125$	~ 1000
		$StSc^{2/3} = 0{\cdot}442\left[\frac{Re}{\epsilon}\right]^{-0{\cdot}31}$	$125 < \frac{Re}{\epsilon} < 5000$	
77	Porous spherical and cylindrical particles	$j_d = 2{\cdot}25\left[\frac{Gd}{\mu}\frac{1}{1-\epsilon}\right]^{-0{\cdot}561}$	wide range	0·60

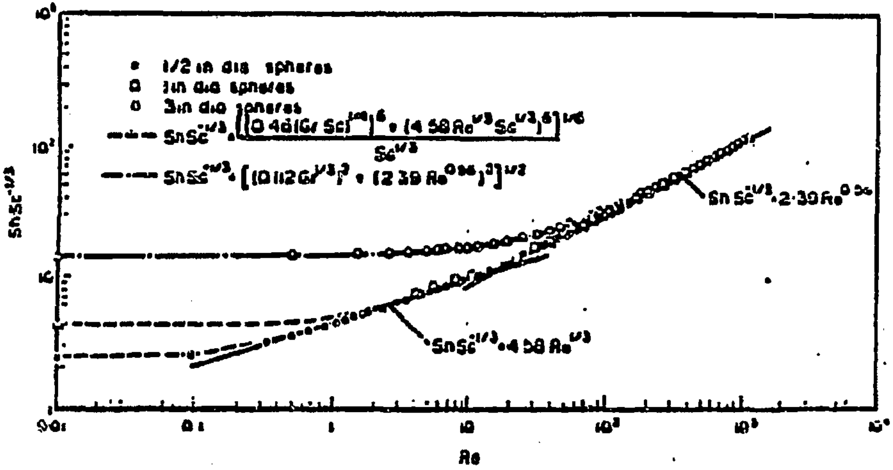

Figure 2-9: Asymptotic correlations for the combined natural and forced convection[51]

2.5 Experimental

The schematic diagram of the experimental apparatus used in this study is shown in Figure 2-10. Liquid carbon dioxide is pumped into the system via a high-pressure Milton-Roy liquid pump. Pressure is controlled by using a back pressure regulator and pressure fluctuation is dampened with an on-line surge tank. The system consists of a preheater which allows the solvent to reach the desired temperature and the extraction vessel 171 cm^3 in volume, 14.6 cm in length and 3.87 in diameter. The extraction vessel is packed with naphthalene pellets which have been made from pure naphthalene using a die. The height of the packing in the bed can be changed by using inert packing at the bottom and the top of the bed. The inert packing material being used is glass beads with size similar to that of the pellets. Another advantage in using the inert pellets is to get rid of end effects in the packed bed being used as the extractor. Pressure at the inlet of extractor is measured using a pressure transducer. The temperature of the extractor is measured at the inlet.

The fluid mixture coming out of the extractor is depressurized to atmospheric pressure by passing it through a heated metering valve and a back pressure regulator. The instantaneous flow rate of the gas leaving the extractor is measured using a rotameter and the total amount of gas flow is measured with a calibrated wet-test meter.

The mass of precipitated solid is found as described below. With this value and total amount of gas flow through wet-test meter, the mole fraction of solids in the supercritical fluid can be readily determined. The temperature and pressure in wet-test meter are also measured.

The sample collectors are high pressure bombs which are kept at room temperature by two 200 watt resistance heaters. Each vessel contains toluene

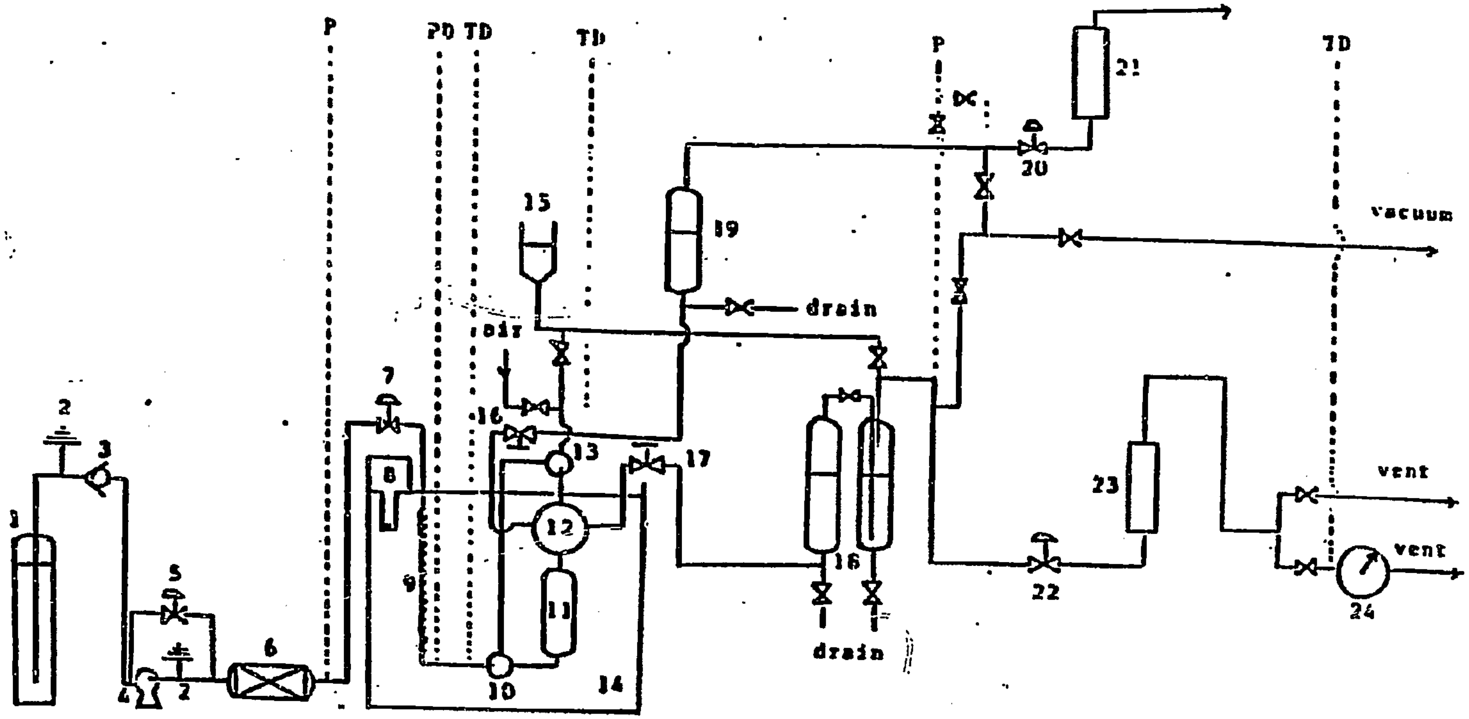

1. Cylinder
2. Relief valve
3. Check valve
4. Liquid pump
5. Back pressure regulator
6. Surge tank
7. Pressure regulator
8. Temperature controller
9. Preheater
10. Three-way valve
11. Extractor
12. Four-way valve
13. Three-way valve
14. Water bath
15. Solvent tank
16. Metering valve
17. Metering valve
18. Sample tanks
19. Solid trap
20. Back pressure regulator
21. Rotameter
22. Back pressure regulator
23. Rotameter
24. Wet test meter

P: Pressure gauge
PD: Pressure transmitter to Data logger
TD: Thermocouple to Data logger

Figure 2-10: Schematic diagram of the experimental apparatus of SCFE which will help dissolve the extract (naphthalene) from the carbon dioxide. These vessels are operated at 300 to 400 psi where the solubility of the solid in the carbon dioxide is at a minimum. The second vessel is redundant and is used to guarantee that all of the extract is collected and to reduce entrainment losses. No naphthalene was found in these vessels during current experiments. To determine the amount of extract collected, the amount of toluene (with dissolved extract) is weighed. A sample of the toluene-extract solution is then injected into a gas chromatograph to determine what portion of the solution is extract. Finally, the bypass, from valve 12 to 16, is designed to insure steady-state flow through the extraction vessel 11.

The whole apparatus is rated for a pressure of 5000 psi. All measured temperatures and pressures are recorded on a data logger at regular time intervals. The parameters that are being studied are:

- Effect of flow rate on solubility of naphthalene in carbon dioxide at different pressures and temperatures.
- Effect of bed height on the mass-transfer coefficient under supercritical conditions.
- Effect of flow rate on the mass-transfer coefficient under supercritical conditions.
- Effect of pressure on the mass-transfer coefficient under supercritical conditions.

The experimental conditions are as follows:

System: Naphthalene - Carbon Dioxide

Pellet Characteristics:

Material: Naphthalene

Shape: Cylindrical

Size: Length (mm) = 4.76

Diameter (mm) = 4.76

Height of Bed (mm): 4.76 - 19.04

Temperature of Bed (^{o}K): 308, 318, 328

Pressure (psi): 1470, 2205, 2940, 3675

Flow Rates (STD. liter/min at 0^{o}C and 1 atm): 4 - 30

Reynolds Number: $10 < Re < 250$

Schmidt Number: $5 < Sc < 12$

Grashof Number: $1.69 \times 10^{6} < Gr < 2.13 \times 10^{7}$

2.6 Plans

This work is divided into two major parts. The first part is to measure mass-transfer coefficients, while the second one is concerned with establishing the mass-transfer correlations under supercritical conditions.

Mass-transfer coefficients in packed beds under standard conditions have been measured using various flow models. However, no study has yet been carried out to estimate the mass-transfer coefficient under supercritical conditions and no mass-transfer correlations under these conditions have been developed.

For this fundamental mass-transfer study under supercritical conditions, naphthalene-CO_2 systems have been chosen due to convenience of getting the values of transport properties such as binary diffusion coefficient, viscosity and density of carbon dioixde from the literature. Experiments are being carried out to investigate the effect of the flow rate of CO_2 on solubility of naphthalene in CO_2. The effect of flow rate on CO_2, temperature, and pressure on mass-transfer coefficients will be determined using the plug flow model and cell model. Then, these mass-transfer coefficient data will be used to developed mass-transfer correlations analogous to those shown in the previous section which would be useful in designing separation units. Finally, these correlations for solid-supercritical fluid will be compared with mass-transfer correlations for solid-gas and/or solid-liquid systems, depending upon three different flow conditions, respectively (natural, forced, and combined natural and forced convection).

Results

Work for current period (July 1 - September 30, 1987).

Two layers of naphthalene pellets were used to get mass transfer coefficients in a packed bed. We operated our system continuously for about two minutes at 35°C and 100 atm for several flow rates of carbon dioxide. The resultant data of mass transfer coefficients were shown in Table 2-5. These data were compared with ones obtained by using one layer of naphthalene pellets (Table 6) and were given in Figures 2-11 and 2-12.

Mass transfer coefficients were calculated by both of the ideal plug flow model and the cell model. Its comparison was given in Figures 2-13 and 2-14 for 1 layer of naphthalene pellets, and Figures 2-15 and 2-16 for 2 layers of naphthalene pellets, respectively. From these graphs, we can find that the value of mass transfer coefficients by the cell model is approximately 12% higher than the one by the ideal plug flow model. This difference can be explained by the fact that the cell model takes account of the effect of the axial dispersions on mass transfer coefficient in a packed bed. More data is needed to determine the true correlation between dimensionless groups (Sh, Sc, Re, Gr). A wider range of experimental conditions will be studied in the following quarter.

TABLE 2-5

Results for Mass Transfer Coefficients and jd vs. Re Correlation at 35°C and 100 atm for 1 Layer of Naphthalene Pellets

				Mass Transfer Coefficient ky x 10^4			Mass Transfer Factor Jd	
Run No.	Superficial Flow Rate (l/min) at 0°C .1 atm	Exit Mole Fraction yx 10^3	Mass Velocity G·x 10^2	Ideal Plug Ideal Model	Cell Model	Reynolds Number Re	Ideal Plug Ideal Model	Cell Model
1-5	24.158	3.0344	6.84	1.782	1.948	55.77	0.4393	0.4802
1-6	21.922	3.1736	6.21	1.725	1.895	50.61	0.4685	0.5146
1-2	19.324	3.4816	5.48	1.744	1.938	44.61	0.5373	0.5970
1-1	17.798	3.6258	5.05	1.710	1.911	41.09	0.5719	0.6390
1-7	15.818	3.8852	4.49	1.695	1.914	36.51	0.6376	0.7199
1-3	14.009	4.3036	3.98	1.779	2.044	32.34	0.7553	0.8679
1-8	12.922	4.3182	3.67	1.652	1.900	29.83	0.7603	0.8743
1-4	10.906	4.8020	3.10	1.688	1.985	25.18	0.9201	1.0818
1-9	9.539	5.0142	2.72	1.605	1.907	22.02	0.999	1.1880
1-10	7.815	5.5023	2.23	1.592	1.941	18.04	1.2099	1.4752

TABLE 2-6

Results for Mass Transfer Coefficients and Jd vs. Re Correlation at 35°C and 100 atm for 2 Layers of Naphthalene Pellets

				Mass Transfer Coefficient $k_y \times 10^4$			Mass Transfer Factor Jd	
Run No.	Superficial Flow Rate (l/min) at 0°C, 1 atm	Exit Mole Fraction $y \times 10^3$	Mass Velocity $G \times 10^2$	Ideal Plug Flow Model	Cell Model	Reynolds Number Re	Ideal Plug Flow Model	Cell Model
2-1	22.109	5.8010	6.0778	1.6692	1.9241	45.967	0.4938	0.5692
2-7	19.902	5.8085	5.4597	1.2550	1.4097	41.016	0.4124	0.4633
2-5	18.231	5.3838	5.0065	1.3279	1.5071	36.454	0.4764	0.5407
2-4	16.307	5.6156	4.4805	1.1724	1.3419	33.882	0.4702	0.5382
2-2	15.021	5.3674	4.1243	1.0368	1.1760	30.786	0.4514	0.5120
2-3	12.765	6.8045	3.5194	1.2418	1.4969	26.734	0.6362	0.7669
2-8	6.136	8.5764	1.7003	1.0204	1.4000	12.676	1.0877	1.4924

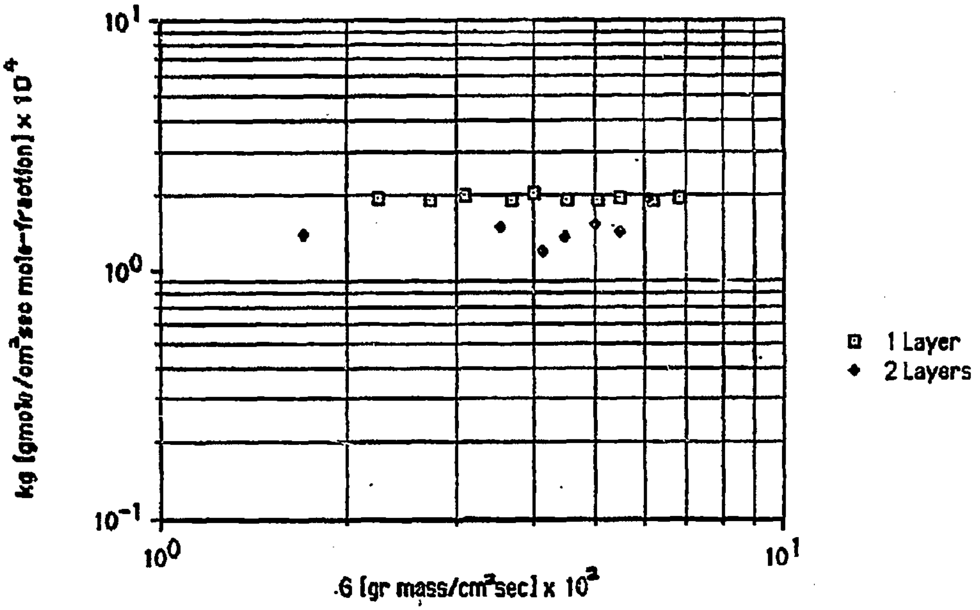

Figure 2-11 **Correlation between kg and G at 35 C and 100 atm by Cell model**

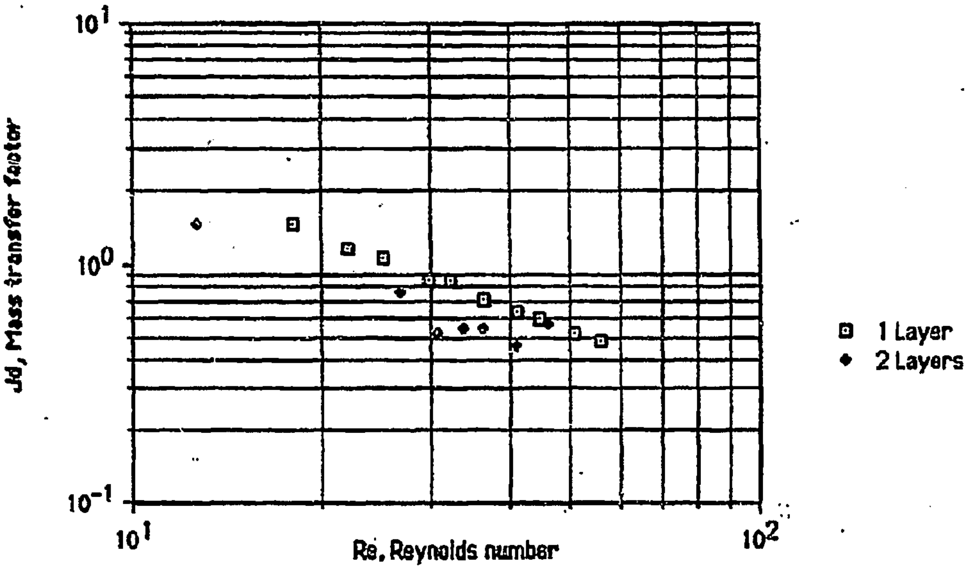

Figure 2- 12 **Relationship between Jd and Re at 35C and 100 atm by cell model**

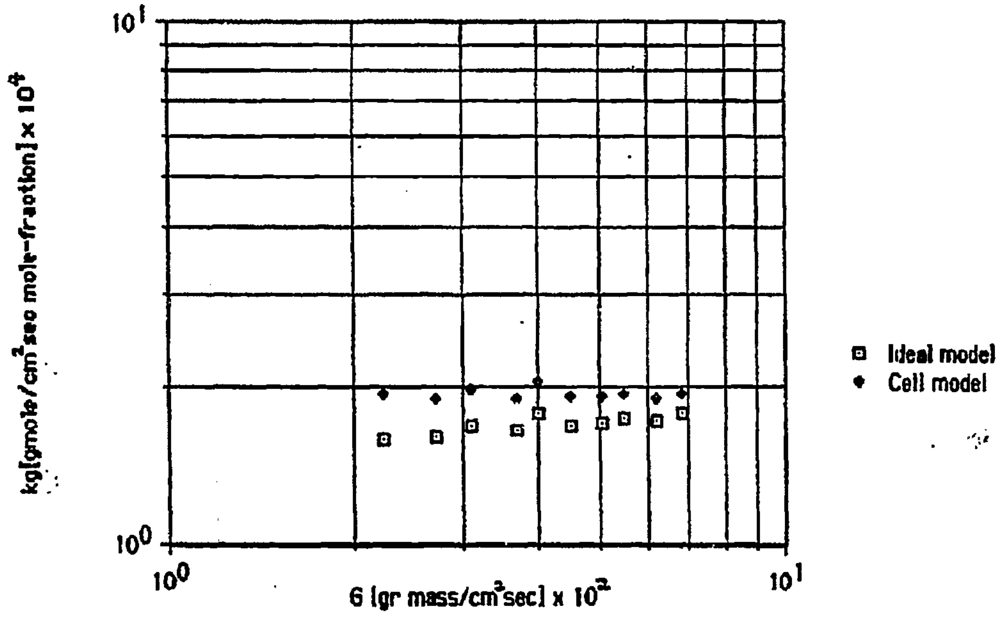

Figure 2-13 Correlation between kg and G at 35 C and 100 atm for 1 layer

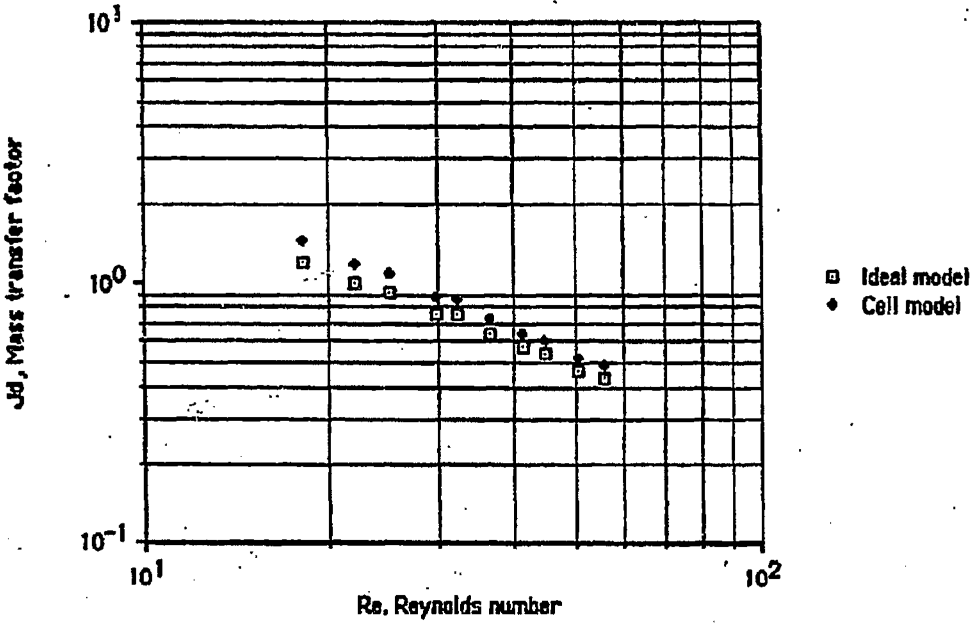

Figure 2-14 Relationship between Jd and Re at 35 C and 100 atm for 1 layer

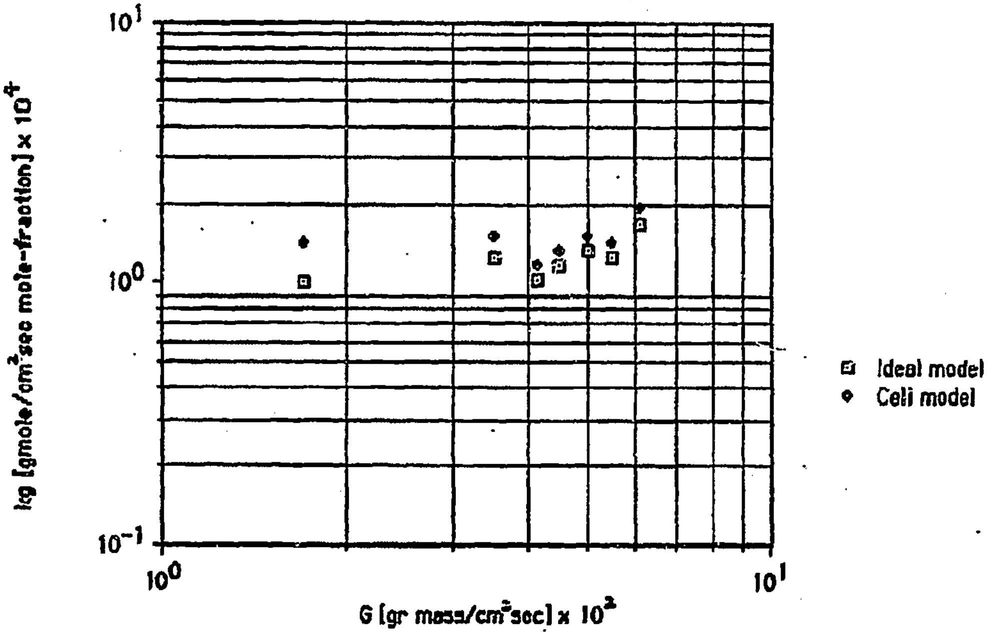

Figure 2-15 Correlation between kg and G at 35 C and 100 atm for 2 layers

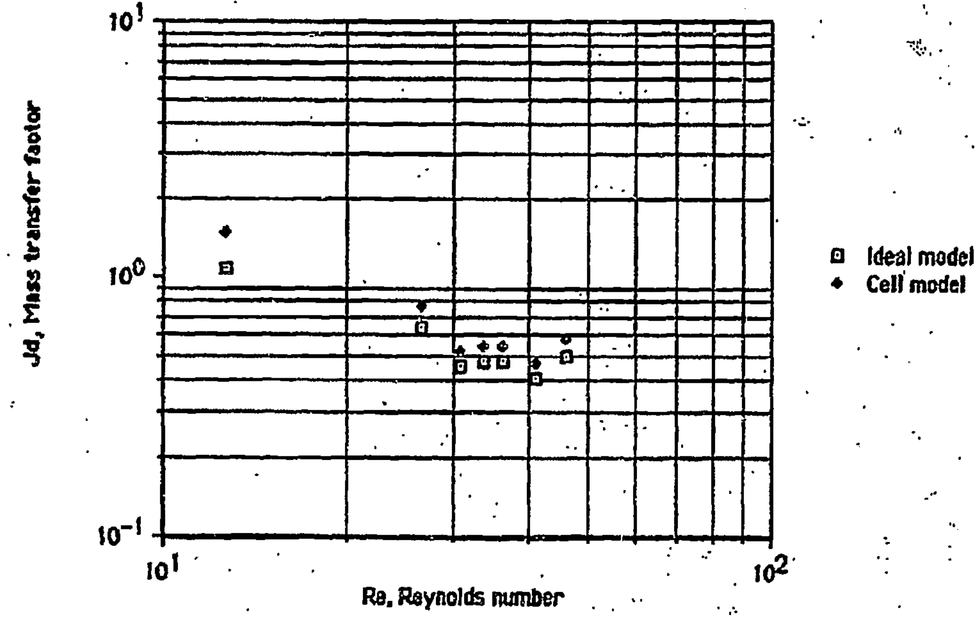

Figure 2-16 Relationship between Jd and Re at 35 C and 100 atm for 2 layers

NOMENCLATURE

a : System parameter in Peng-Robinson equation of state
a_s : Surface area of pellets per unit volume of extractor [cm^2/cm^3]
A_p : Surface area of single particle [cm^2]
A_T : Total surface area of pellets in extractor [cm^2]
b : System parameter in Peng-Robinson equation of state
C : Concentration of solute [$gmole/cm^3$]
d_p : Diameter of sphere possessing the same surface area as a piece of packing [cm]
D_v : Molecular diffusivity [cm^2/sec]
E_a : Axial dispersion coefficient [cm^2/sec]
E_r : Radial dispersion coefficient [cm^2/sec]
f_i^s : Fugacity of component i in solid phase [atm]
f_i^v : Fugacity of component i in vapor phase [atm]
g : Gravitational acceleration [cm/s
G : Mass velocity [g/cm^2sec]
$\bar{G}_{My}$: Average molal mass velocity [$gmole/cm^2sec$]
G_{My} : Molal mass velocity [$gmole/cm^2sec$]
Gr : Grashof number = $d^3 g\rho\Delta\rho/\mu^2$
j_d : Mass transfer factor = $ShRe^{-1}Sc^{-1/3}$
k_c : Mass transfer coefficient = k_yC [cm/sec]
k_{ij} : Binary interaction parameter
k_y : Mass transfer coefficient [$gmole/cm^2sec$ mole-fraction]
L_T : Total height of bed [cm]
M_{av} : Average molecular weight [g/gmole]
n : Number of perfect mixers

N_A : Molal flux of solute [gmole/cm^{2}sec]

P : Total pressure [atm]

P_c : Critical pressure [atm]

Pe : Peclet number = $u_s d_p/D_v$

$P_{e,a}$: Axial peclet number = ud_p/E_a

P_1^s : Saturation (Vapor) pressure of pure solid [atm]

R : Gas constant = 0.08205 [atm liter/gmole °K]

Re : Reynolds number = $\rho d_p u_s/\mu$

S : Cross section area of packed bed [cm^2]

Sc : Schmidt number = $\mu/\rho D_v$

Sh : Sherwood number = $k_c d_p/D_v$

T : Absolute temperature

T_c : Critical temperature [°K]

T_r : Reduced temperature

T_ε : Tortuosity of bed

u : Interstitial velocity [cm/sec]

u_s : Superficial velocity [cm/sec]

V_T : Total molal flow rate [gmole/sec]

V' : Molal flow rate of inert component [gmole/sec]

y_A : Mole fraction of component A

y_A^* : Equilibrium mole fraction of component of A

y_i : Mole fraction of component A in stream outgoing from ith cell

Z : Compressibility factor

Greek Letters

ε : Void fraction

ϕ_{iv} : Fugacity coefficient of component i in vapor phase

ϕ_{is}^{S} : Fugacity coefficient of component i in solid phase at saturaction pressure P_i^S

γ_i^{∞} : Activity coefficient at infinite dilution

μ : Viscosity [g/cm sec]

ρ : Density [g/cm^3]

BIBLIOGRAPHY

1. Chang, H. and Morrell, D.G., "Solubilities of Methoxy-1-Tetralone and Methyl Nitrobenzoate Isomers and their Mixtures in Supercritical Carbon Dioxide," J. Chem. Eng. Data, Vol. 30, 1985, pp.74.

2. Irani, C.A. and Funk, E.W., Separation Using Supercritical Gases, CRC Hand Book, CRC Press, Boca Raton, FL, 1977, pp. 171, Ch. Part A.

3. Paul, P.F.M. and Wise, W.S., The Properties of Gases Extraction, Mills and Boom Ltd., London, 1971.

4. Sirtl, W., "Examples of Cost Determinations," High Pressure Extraction Symposium, NOVA-WERKE AG. Effretikon, Switzerland, August 1979.

5. Colburn, A.P., "A Method of Correlating Forced Convection Heat Transfer Data and a Comparison with Fluid Friction," AIChE J., Vol. 29, 1933, pp. 174.

6. Chilton, T.H. and Colburn, A.P., "Mass-Transfer (Absorption) Coefficients (Prediction from Data on Heat Transfer and Fluid Friction)," Ind. Eng. Chem., Vol. 26, 1934, pp. 1183.

7. Gupta, A.S. and Thodos, G., "Mass and Heat Transfer in the Flow of Fluids through Fixed and Fluidized Beds of Spherical Particles," AIChE J., Vol. 8, 1962, pp. 608.

8. Wilson, E.J. and Geankoplis, C.J., "Liquid Mass-Transfer at Very Low Reynolds Numbers in Packed Beds," Ind. Eng. Chem. Fund., Vol. 5, 1966, pp. 9.

9. Storck, A. and Coeuret, F., "Mass-Transfer Between a Flowing Liquid and a Wall or an Immersed Surface in Fixed and Fluidized Beds," Chem. Eng. J., Vol. 20, 1980, pp. 149.

10. Pfeffer, R., "Heat and Mass Transfer in Multiparticle Systems," Ind. Eng. Chem. Fund., Vol. 3, 1964, pp. 380.

11. Bradshaw, R.D. and Bennett, C.O., "Fluid-Particle Mass Transfer in a Packed Bed," AIChE J., Vol. 7, 1961, pp. 48.

12. Hannay, J.B., "On the Solubility of Solids in Gases," Proc. Roy. Soc. (London), Vol. 30, 1880, pp. 484.

13. Hannay, J.B. and Hogarth, J., "On the Solubility of Solids in Gases," Proc. Roy. Soc. (London), Vol. 29, 1879, pp. 324.

14. Hannay, J.B. and Hogarth, J., "On the Solubility of Solids in Gases," Proc. Roy. Soc. (London), Vol. 30, 1880, pp. 178.

15. Buchner, E.H., "Flussige Kohlensaure als Losungsmittel," Z. Physik. Chem., Vol. 54, 1906, pp.665.

16. Centnerszwer, M., "Uber Kritische Temperaturen der Losungen," Z. Physik. Chem., Vol. 46, 1903, pp. 427.

17. Sage, B.H., Webster, D.C. and Lacey, W.N., "Phase Equilibria in Hydrocarbon Systems: XVI. Solubility of Methane in Four Light Hydrocarbons," Ind. Eng. Chem., Vol. 28, 1936, pp. 1045.

18. Kay, W.B., "Liquid-Vapor Phase Equilibrium Relations in the Ethane-n-Heptane System," Ind. Eng. Chem., Vol. 30, 1938, pp. 459.

19. Messmore, H.E., U.S. Pat. 2,420,185, 1943.

20. Maddocks, R.R. and Gibson, "Supercriticle Extraction of Coal," J. Chem. Eng. Progr., Vol. 73, 1977, pp. 59.

21. Tugrul, T. and Oclay, A., "Supercritical Gas Extraction of Two Lignites," Fuel, Vol. 57, 1978, pp. 415.

22. Bartle, K.D. et al., "Chemical Nature of a Supercritical-Gas Extract of Coal at 350°C," Fuel, Vol. 54, 1975, pp. 227.

23. Barton, P. and Fenske, M.R., "Hydrocarbon Extraction of Saline Water," Ind. Eng. Chem. Process Des., Vol. 9, 1970, pp. 18.

24. Hubert, P. and Vitzhum, O., "Fluid Extraction of Hops, Spices and Tobacco with Supercritical Gases," Agnew Chem. Inc., Vol. 17, 1978, pp. 710, England.

25. Modell, M., deFelippi, R.P. and Krukonis, V., "Regeneration of Activated Carbon with Supercritical Carbon Dioxide," Am. Chem. Soc. Meet., Miami, September 1978.

26. Modell, M. et al., "Supercritical Fluid Regeneration of Activated Carbon," 87th Nat. Meet. Am. Inst. Chem. Eng., 1979.

27. Diepen, G.A.M. and Scheffer, F.E.C., "The Solubility of Naphthalene in Supercritical Ethylene II," J. Phys. Chem., Vol. 57, 1953, pp. 575.

28. Tsekhanskaya, Yu., V., Iomtev, M.B. and Mushkina, E.V., "Solubility of Naphthalene in Ethylene and Carbon Dioxide under Pressure," Russ. J. Phys. Chem., Vol. 38, 1964, pp. 1173.

29. Modell, M. et al., ".", 72nd AIChE J. Annual Meeting, San Francisco, CA, Nov., 1979.

30. Mackay, M.E. and Paulaitis, M.E., "Solid Solubilities of Heavy Hydrocarbons in Supercritical Solvents," Ind. Chem. Fund., Vol. 18, 1979, pp. 149.

31. Peng, D.Y. and Robinson, D.B., "A New Two-Constant Equation of State," Ind. Eng. Chem. Func., Vol. 15, 1976, pp. 59.

32. Balenovc, Z., Myer, M.N., Giddings, J.E., "Binary Diffusion in Dense Gases to 1360 atmm by Chromatogrphic Peak-Broadening Method," J. Chem. Phys., Vol. 52, 1970, pp. 915.

33. Feist, R. and Schneider, G.M., "Determination of Binary Diffusion Coefficient of Benzene, Phenol, Naphthalene and Caffeine in Supercritical CO_2 between 308 and 333 °K in the Pressure Range 80 to 160 Bar with Supercritical Fluid Chromatography (SFC)," J. Separation Sci. and Tech., Vol. 17, 1982, pp. 261.

34. Waid, I. and Schneider, G.M., "Determination of Binary Diffusion Coefficients of the Benzene and Some Alkylbenzenes in Supercritical CO_2 between 308 and 320°K in the Pressure Range 80 to 160 Bar with Supercritical Fluid Chromatography," Ber Bunsenges. Phys. Chem., Vol. 83, 1979, pp. 969.

35. Paulaitis, M.E., Krukonis, V.J., "Supercritical Fluid Extraction," Rev. Chem. Eng., Vol. 1, 1983, pp. 179.

36. Stephen, K. and Lucas, K., Viscosity of Dense Gas, Plenum Press, NY, 1979.

37. Carberry, J.J. and Bretton, R.H., "Axial Dispersion of Mass in Flow through Fixed Beds," AIChE J., Vol. 4, 1958, pp. 367.

38. Chung, S.F. and Wen, C.Y., "Longitudinal Dispersion of Liquid Flowing through Fixed and Fluidized Beds," AIChE J., Vol. 14, 1968, pp. 857.

39. Ebach, E.A. and White, R.R., "Mixing of Fluids Flowing through Beds of Packed Solids," AIChE J., Vol. 4, 1958, pp. 161.

40. Cholette, A. and Cloulier, L., ".", Can. J. Chem. Eng., Vol. 37, 1959, pp. 105.

41. Danckwerts, P.V., "Continuous Flow System (Distribution of Residence Time)," Chem. Eng. Sci., Vol. 2, 1953, pp. 1.

42. Wen, C.Y. and Fan, L.T., Models for Flow Systems and Chemical Reactors, Marcel Dekker, Inc., NY, 1975.

43. Sherwood, T.K. et al., Mass-Transfer, McGraw-Hill Inc., NY, 1975, pp. 136.

44. Kramers, H. and Alberda, G., "Frequency Response Analysis of Continyuous Flow Systems," Chem. Eng. Sci., Vol. 2, 1953, pp. 173.

45. Adler, R.J. and Hovorka, R.B., ".", JACC, Denver, 1961.

46. Deans, H.A. and Lapidus, L., "A Computational Model for Predicting and Correlating the Behavior of Fixed Bed Reactor: 1. Derivation of Model for Non-Reactive Systems," AIChE J., Vol. 6, 1960, pp. 656.

47. Levenspiel, O., "Mixed Models to Represent Flow of Fluids through Vessels," Can. J. Chem. Eng., Vol. 40, 1962, pp. 135.

48. Levenspiel, O., Chemical Reaction Engineering, John Wiley and Sons, NY, 1962.

49. Eckert E.R.G., Introduction to Heat and Mass Transfer, McGraw-Hill Inc., NY, 1950.

50. Debenedetti, P.G. and R.C. Reid, "Diffusion and Mass-Transfer in Supercritical Fluids," AIChE J., Vol. 32, 1986, pp. 2034.

51. Karabelas, A.J. et al., "Use of Asymptotic Relations to Correlate Mass-Transfer Data in Packed Beds," Chem. Eng. Sci., Vol. 26, 1971, pp. 1581.

52. Petrovic, L.J. and Thodos, G., "Mass-Transfer in the Flow of Gases through Packed Bed," Ind. Chem. Fund., Vol. 7, 1968, pp. 274.

53. Garner, F.H. and Grafton, R.W., ".", Proc. Roy. Soc. (London), Vol. A224, 1954, pp. 64.

54. McHugh, M. and Paulaitis, M.E., "Solid Solubilities of Naphthalene and Biphenyl in Supercritical Carbon Dioxide," J. Chem. Eng. Data, Vol. 25, 1980, pp. 326.

55. Goto, S. et al., "Mass Transfer in Packed Beds with Two-Phase Flow," Ind. Eng. Process Des. Dev., Vol. 14, 1975, pp. 473.

56. Morozov, V.S. and Vinkler, E.G., "Measurement of Diffusion Coefficients of Vapors of Solids in Compressed Gases. I. Dynamic Method for Measurement of Diffusion Coefficients," Russ. J. Phys. Chem., Vol. 49, 1975, pp. 1404.

57. Vinkler, E.G. and Morozov, V.S., "Measurement of Diffusion Coefficients of Vapors in Compressed Gases. II. Diffusion Coefficients of Naphthalene in Nitrogen and In Carbon Dioixde," Russ. J. Phys. Chem., Vol. 49, 1975, pp. 1405.

58. Iomtev, M.B. and Tsekhanskaya, Yu. V., "Diffusion of Naphthalene in Compressed Ethylene and Carbon Dioxide," Russ. J. Phys. Chem., Vol. 38, 1964, pp. 485.

59. Tsekhanskaya, Yu. V., "Diffusion in the System p-Nitrophenol-Water in the Critical Region," Russ. J. Phys. Chem., Vol. 42, 1968, pp. 532.

60. Schneider, G.M., "Chem. Thermodynamics Specialists Periodical Report," Tech. Report, Chem. Soc., London, 1978, Vol. 2, Chap. 4.

61. Gamson, B.W. et al., "Heat, Mass and Momemtum Transfer in the Flow of Gases through Granular Solids," AIChE J., Vol. 39, 1943, pp. 1.

SATISFACTION GUARANTEED

NTIS strives to provide quality products, reliable service, and fast delivery. Please contact us for a replacement within 30 days if the item you receive is defective or if we have made an error in filling your order.

- **E-mail: info@ntis.gov**
- **Phone: 1-888-584-8332 or (703)605-6050**

Reproduced by NTIS

National Technical Information Service
Springfield, VA 22161

This report was printed specifically for your order from nearly 3 million titles available in our collection.

For economy and efficiency, NTIS does not maintain stock of its vast collection of technical reports. Rather, most documents are custom reproduced for each order. Documents that are not in electronic format are reproduced from master archival copies and are the best possible reproductions available.

Occasionally, older master materials may reproduce portions of documents that are not fully legible. If you have questions concerning this document or any order you have placed with NTIS, please call our Customer Service Department at (703) 605-6050.

About NTIS

NTIS collects scientific, technical, engineering, and related business information – then organizes, maintains, and disseminates that information in a variety of formats – including electronic download, online access, CD-ROM, magnetic tape, diskette, multimedia, microfiche and paper.

The NTIS collection of nearly 3 million titles includes reports describing research conducted or sponsored by federal agencies and their contractors; statistical and business information; U.S. military publications; multimedia training products; computer software and electronic databases developed by federal agencies; and technical reports prepared by research organizations worldwide.

For more information about NTIS, visit our Web site at http://www.ntis.gov.

NTIS

Ensuring Permanent, Easy Access to U.S. Government Information Assets

U.S. DEPARTMENT OF COMMERCE
Technology Administration
National Technical Information Service
Springfield, VA 22161   (703) 605-6000